Available online at www.sciencedirect.com

SCIENCE DIRECT

Biochimica et Biophysica Acta 1707 (2005) 1–23

BIOCHIMICA ET BIOPHYSICA ACTA
BBA

http://www.elsevier.com/locate/bba

Review

Light-driven enzymatic catalysis of DNA repair: a review of recent biophysical studies on photolyase

Stefan Weber*

Institute of Experimental Physics, Free University Berlin, Arnimallee 14, 14195 Berlin, Germany

Received 28 April 2003; accepted 2 February 2004
Available online 8 May 2004

Abstract

More than 50 years ago, initial experiments on enzymatic photorepair of ultraviolet (UV)-damaged DNA were reported [Proc. Natl. Acad. Sci. U. S. A. 35 (1949) 73]. Soon after this discovery, it was recognized that one enzyme, photolyase, is able to repair UV-induced DNA lesions by effectively reversing their formation using blue light. The enzymatic process named DNA photoreactivation depends on a non-covalently bound cofactor, flavin adenine dinucleotide (FAD). Flavins are ubiquitous redox-active catalysts in one- and two-electron transfer reactions of numerous biological processes. However, in the case of photolyase, not only the ground-state redox properties of the FAD cofactor are exploited but also, and perhaps more importantly, its excited-state properties. In the catalytically active, fully reduced redox form, the FAD absorbs in the blue and near-UV ranges of visible light. Although there is no direct experimental evidence, it appears generally accepted that starting from the excited singlet state, the chromophore initiates a reductive cleavage of the two major DNA photodamages, cyclobutane pyrimidine dimers and (6–4) photoproducts, by short-distance electron transfer to the DNA lesion. Back electron transfer from the repaired DNA segment is believed to eventually restore the initial redox states of the cofactor and the DNA nucleobases, resulting in an overall reaction with net-zero exchanged electrons. Thus, the entire process represents a true catalytic cycle.

Many biochemical and biophysical studies have been carried out to unravel the fundamentals of this unique mode of action. The work has culminated in the elucidation of the three-dimensional structure of the enzyme in 1995 that revealed remarkable details, such as the FAD-cofactor arrangement in an unusual U-shaped configuration. With the crystal structure of the enzyme at hand, research on photolyases did not come to an end but, for good reason, intensified: the geometrical structure of the enzyme alone is not sufficient to fully understand the enzyme's action on UV-damaged DNA. Much effort has therefore been invested to learn more about, for example, the geometry of the enzyme–substrate complex, and the mechanism and pathways of intra-enzyme and enzyme ↔DNA electron transfer. Many of the key results from biochemical and molecular biology characterizations of the enzyme or the enzyme–substrate complex have been summarized in a number of reviews. Complementary to these articles, this review focuses on recent biophysical studies of photoreactivation comprising work performed from the early 1990s until the present.

Keywords: DNA repair; Flavin adenine dinucleotide; Cyclobutane pyrimidine dimer; (6–4) Photoproduct; Electron transfer; Radical-pair mechanism; Superexchange

1. Ultraviolet (UV) radiation damage to DNA and its repair by photoreactivation

Solar UV radiation in the UV-B (290–320 nm) and UV-C (100–290 nm) spectral regions has mutagenic, carcinogenic, and lethal effects on living organisms [1]. There is evidence that with the progressing depletion of the atmospheric ozone layer, these effects will have increasingly serious consequences for the biosphere [2–5]. The most significant cellular target of UV is DNA. When DNA is exposed to radiation at wavelengths approaching its absorption maximum at around 260 nm, adjacent pyrimidines within the same DNA strand may become covalently linked by the formation of mostly

* Tel.: +49-30-838-56139; fax: +49-30-838-56046.
E-mail address: Stefan.Weber@physik.fu-berlin.de (S. Weber).

0005-2728/$ - see front matter © 2004 Elsevier B.V. All rights reserved.
doi:10.1016/j.bbabio.2004.02.010

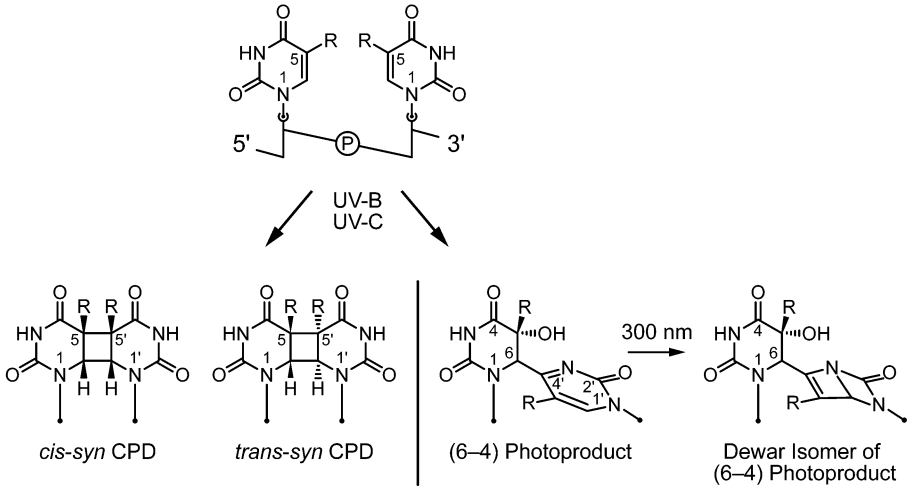

Fig. 1. The structures of the most mutagenic UV-induced DNA lesions. R denotes either H in uracil (U) or CH_3 in thymine (T). The *cis–syn* CPD is a diastereomer of the *trans–syn* CPD.

(70–80%) four-membered ring structures referred to as cyclobutane pyrimidine dimers (CPDs)[1] and, to a lesser extent (20–30%), of pyrimidine (6–4) pyrimidone photoproducts ((6–4)PPs)[2] [1] (see Fig. 1). The photochemical generation of (6–4)PPs involves the transfer of the hydroxyl group at C(4′) of the 3′-base, via an oxetane intermediate, to the C(5) position of the 5′-base. The (6–4)PP is almost quantitatively converted to its Dewar isomer by irradiation with light of 300–350 nm. Hence, under natural conditions, a significant fraction of the (6–4)PP is expected to be in its Dewar isomer form [6]. The exact yields and the type of UV-induced damage depend on the sequence and structure of DNA [7–10], the DNA curvature [11] and the folding of DNA into nucleosomes [12,13]. Sequences that facilitate DNA bending and unwinding are favorable sites for damage formation. Thus, CPDs form in higher yields in single-stranded DNA and at the flexible ends of poly(dA)–(dT) tracts than in their more rigid centers [10,14]. Twelve isomeric forms of CPDs exist; however, only the four with the configurations *cis–syn*, *cis–anti*, *trans–syn*, and *trans–anti* occur with significant yields.

Both types of DNA lesions, CPDs and (6–4)PPs, block the work of DNA/RNA polymerases. This may result in nucleotide misincorporation or may inhibit the polymerase progression during DNA replication or transcription all together [15–18]. CPD formation is thought to be of crucial importance for the initiation of skin cancer [6,19–22], because it was found to be closely linked to the generation of mutations in tumor suppressor genes, such as p53, expressed in UV-induced skin tumors [23,24].

To avoid toxic effects of UV-induced DNA damage and to maintain genetic integrity, most organisms utilize a network of repair mechanisms. Pyrimidine dimers may be mended by nucleotide excision repair [25]. In this type of cellular response to DNA damage, an oligonucleotide containing the lesion is excised from the DNA and the resulting single-strand gap refilled correspondingly. An alternative to the complex multi-step pathway of nucleotide excision repair is photoreactivation, which is an energetically cheaper, more direct, and thus less error-prone way of reversing pyrimidine dimers to their monomeric form. The process is catalyzed by one enzyme, initially called photoreactivating enzyme [26,27], later renamed photolyase [28]. Photoreactivation is a light-dependent process using UV-A (320–400 nm) and blue light (400–500 nm) to monomerize pyrimidine dimers [29–46]. Photolyases are widespread in nature and, for example, have been reported in many vertebrates including fish, reptiles, and marsupials. The human genome has two CRY genes with similarity to photolyase sequences [47–50]. These, however, encode blue-light photoreceptors involved in setting of circadian rhythms [46,51–56] but not in photoreactivation of DNA damage. Additional homologs of DNA-repair photolyases in the human genome have not been detected [57]. Aside from recent reports of transgenic mice [58], it is therefore generally accepted that placental mammals lack photolyase activity [59–61].

2. Classification and spectral properties of photolyases

All photolyases are monomeric proteins with molecular masses in the 53–66 kDa range (454–614 amino acid residues) depending on the organism [29]. Photolyases are

[1] Throughout the text the abbreviation Base (1)◇Base (2) is also used for CPDs (e.g., T◇T), where the "◇" represents the cyclobutane ring that links the two bases 1 and 2. As this review is mainly focused on the *cis–syn* form, which is the main substrate in DNA photorepair, the qualifier "*cis–syn*" shall be dropped for convenience except for cases where the configuration of the CPD is relevant.

[2] The abbreviation Base(1)-64-Base(2) (e.g., T-64-C) will be used in cases where the base composition of the (6–4)PP is relevant. "-64-" represents the σ-bond linking C(6) on the 5' base and C(4') on the 3' base.

distinguished by their different substrate specificity: CPD photolyase (also called DNA photolyase) binds and repairs CPD lesions in single-strand or double-helical DNA, whereas (6–4) photolyase reverses (6–4)PP-damages in DNA. CPD photolyases are further classified into two classes, I and II, based on their amino acid sequence similarity [62–64]. Class-I photolyases are found in many microbial organisms, whereas most of the class-II photolyases have been identified and cloned from higher organisms including the animals *Carassius auratus* (goldfish) [65], *Drosophila melanogaster* (fruit fly) [62,66], *Potorous tridactylis* (rat kangaroo) [62], *Oryzias latipes* (killifish) [62], and the plants *Arabidopsis thaliana* [67–69], *Cucumis sativus* (cucumber) [70] and *Oryza sativa* (rice) [71], but also from the archaebacterium *Methanobacterium thermoautotrophicum* [62], the eubacterium *Myxococcus xanthus* [72], and the single-celled alga *Chlamydomonas* [73]. Through recent genome-sequencing efforts, it has been discovered that also some poxviruses encode functional CPD photolyases of type II [74,75]. A photolyase gene from the plant *Sinapis alba* (white mustard) [76], however, is more closely related to the (microbial) class-I than to the (higher eukaryotes) class-II photolyases [62].

All known photolyases contain stoichiometric amounts of non-covalently bound flavin adenine dinucleotide (FAD) as redox-active cofactor [62,68,71,77–84]. Nevertheless, no obvious amino acid sequence homology to other classes of flavoproteins exists, perhaps because the enzymatic activity of photolyases depends on the photoexcited state of FAD in the two-electron reduced form, $FADH^-$ (see Fig. 2), whereas the vast majority of other proteins with flavin chromophores utilizes their ground states [85–87]. $FADH^-$ in photolyases has weak absorbance at wavelengths below and vanishing absorbance above 400 nm, thus rendering the catalytically active enzyme nearly colorless to pale yellow. A second (also non-covalently bound) chromophore functions as an antenna to increase the absorption cross-section of the enzyme and to extend its absorbance to longer wavelengths.

The class-I photoreactivating enzyme is further categorized according to the light-harvesting cofactor into either a folate- or a deazaflavin-type, with 5,10-methenyltetrahydrofolylpolyglutamate (MTHF) or 8-hydroxy-5-deazaflavin (8-HDF) as second chromophore, respectively. MTHF alone has maximum absorbance at 360 nm. When bound to the photolyase enzyme, its absorption is considerably red-shifted to 384 nm due to constraints imposed by protein–cofactor interactions [88]. The folate class of photolyases, therefore, exhibits maximum catalytic activity at 377–410 nm. It includes enzymes from the gram-negative bacteria *Escherichia coli* [88], *Salmonella typhimurium* [89] and *Vibrio cholerae* [90], the yeast *Saccharomyces cerevisiae* [88,91], and the filamentous fungus *Neurospora crassa* [81,92]. The deazaflavin class has an action spectrum with a maximum in the range from 430 to 460 nm (its absorption maximum of 438 nm is also red-shifted compared to the peak absorbance at 420 nm of deazaflavin in isotropic solution) and includes photolyases from the cyanobacterium *Anacystis nidulans* [80,93], the gram-positive bacterium (actinomycete) *Streptomyces griseus* [94], the green alga *Scenedesmus acutus* [95], and the archae *Halobacterium halobium* [96]. Surprisingly, the amino acid sequences of class-II photolyases share characteristics with both 8-HDF- and MTHF-type photolyases; hence, from sequence comparison, the nature of their second chromophore cannot be deduced. The class-II photolyase from *D. melanogaster*, for example, has FAD and MTHF [82], whereas FAD and 8-HDF were found in the enzyme from *M. thermoautotrophicum* [97].

There are some indications that besides the folate-type and deazaflavin-type photolyases, a third group of the enzyme without a second chromophore also exists. The class-II enzyme from *P. tridactylis* [62] and the class-I enzyme from the thermophilic gram-negative eubacterium *Thermus thermophilus* [84] are two examples where a second, light-harvesting pigment has not (yet) been isolated. In the latter case, however, the putative binding site for this cofactor as determined by X-ray crystallography (see below)

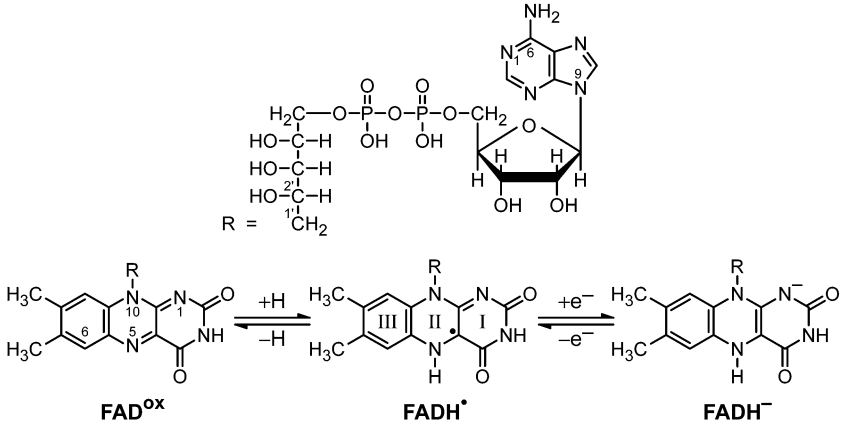

Fig. 2. The redox states of the 7,8-dimethyl isoalloxazine moiety of FAD.

resembles that of an 8-HDF-type photolyase (see also below).

(6–4) Photolyases have been found in *D. melanogaster* [47,98,99], *Xenopus laevis* (South African clawed toad) [83,100], *Crotalus atrox* (rattlesnake) [100], *Danio rerio* (zebrafish) [101], and *A. thaliana* [69,102,103]. In a functional analysis of a *Halobacterium salinarum* deletion mutant in which one of two putative photolyase-gene homologs is deficient, it has been demonstrated that this prokaryotic archae has (6–4)PP-photoreactivating activity [104]. Surprisingly, a gene that was proposed to encode a (6–4) photolyase is also present in the marine hexactinellid sponge *Aphrocallistes vastus* even though this organism typically inhabits water depths where the intensity of UV light is rather low compared to that at the surface [105].

From spectroscopic studies, it is clear that (6–4) photolyases also contain FAD as redox-active cofactor [83,106], which can be present in three oxidative states of flavin: fully oxidized, FAD^{ox}, neutral radical, $FADH^{\bullet}$, and fully reduced, $FADH^{-}$ (see Fig. 2). In semi-purified fractions of *X. laevis* (6–4) photolyase, an absorption peak at 416 nm has been observed and assigned to the second chromophore, presumably MTHF, which, however, is lost upon further purification of the enzyme [106]. A fluorescent species with an excitation maximum at 360 nm and an emission maximum at 440 nm has been observed by fluorescence spectroscopy at pH 10 upon denaturing *D. melanogaster* (6–4) photolyase [107]. Taken together with the fact that neither *D. melanogaster* nor *E. coli* (the organism in which the (6–4) photolyase enzyme was overexpressed) can synthesize deazaflavin [108], it was concluded that (6–4) photolyases utilize MTHF as light-harvesting pigment.

3. CPD photolyase

3.1. Structure of photolyases

In a landmark contribution by Park et al. [109], the three-dimensional structure of the class-I CPD photolyase from *E. coli* determined by X-ray crystallography at 2.3-Å resolution has been presented (see Fig. 3). Subsequently, the crystal structure at 1.8 Å of the (class-I) 8-HDF-type CPD photolyase from *A. nidulans* was elucidated by Tamada et al. [110]. Both enzymes show a similar backbone structure of their single polypeptide chain, consistent with their conserved function and the very homologous amino acid sequences sharing 39% identical and 13% similar residues. The FAD cofactor is bound to a helical domain. An α/β-domain provides binding sites for the second chromophore. The α/β-domain has a typical nucleotide-binding fold with a five-stranded parallel β-sheet covered on both sides by α-helices.

All amino acid residues that non-covalently bind the flavin cofactor belong to the helical domain. Both the position and conformation of the redox-active FAD are virtually identical in both photolyases. The molecule is bent in a unique U-

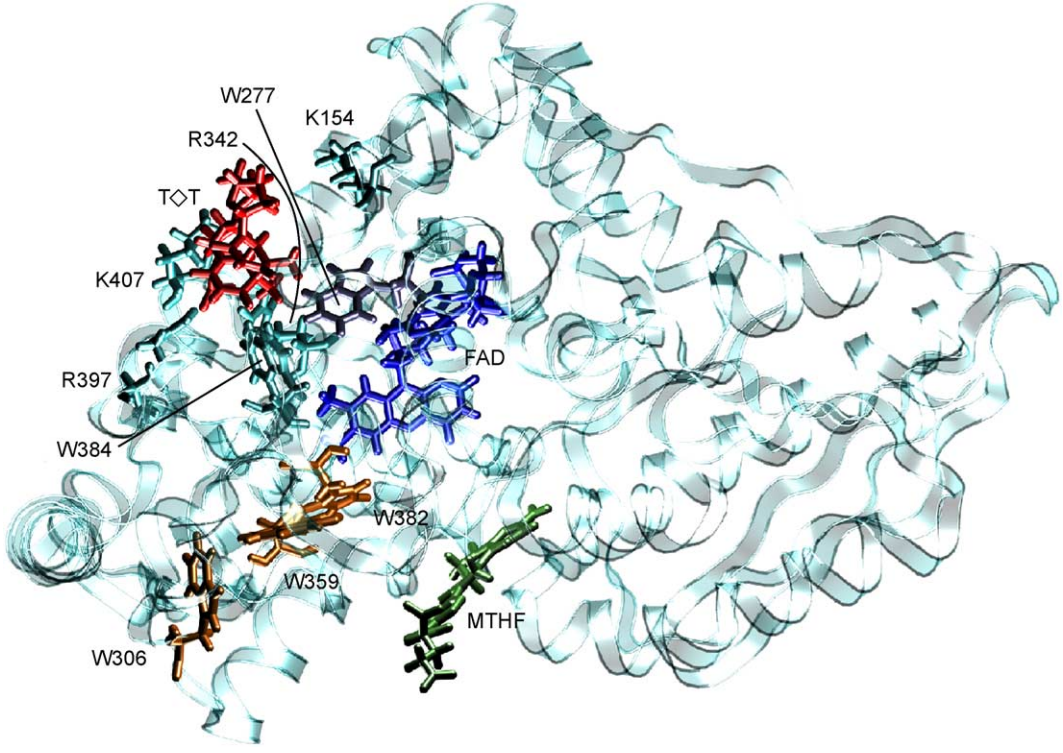

Fig. 3. The structure of *E. coli* CPD photolyase in a ribbon representation. The FAD cofactor and the second chromophore, MTHF, are shown in blue and green, respectively. A thymine dimer at a position that was predicted by molecular modeling calculations [131] is shown in red. Selected amino acid residues that play important functional roles in substrate binding, photoreactivation and photoactivation are also depicted (for details see text).

shaped configuration so that the FAD's 7,8-dimethyl isoalloxazine ring comes in close contact to its adenine ring.

The α/β-domains in the region which recognizes either 8-HDF or MTHF are quite similar in both enzymes. Nevertheless, the photolyase structures reveal completely different binding sites for the light-harvesting chromophores. 8-HDF is more deeply buried in the *A. nidulans* enzyme, whereas MTHF occupies a more surface-exposed site in the *E. coli* photolyase, partially sticking out of the protein. This is a rare example where homologous primary and tertiary structures in closely related proteins accommodate two different types of cofactors at different binding sites. The average separation between 8-HDF and FAD (measured between the centers of their isoalloxazine moieties) in *A. nidulans* photolyase is 17.4 Å, while for MTHF and FAD in *E. coli* photolyase the distance is 16.4 Å (measured between the center of the FAD's isoalloxazine moiety and N(5) of MTHF).

Very recently, the three-dimensional structure of the class-I CPD photolyase from the thermophilic bacterium *T. thermophilus*, determined at 2.1 Å resolution, has also been reported by Komori et al. [111]. The crystal structure revealed a large cavity inside the cleft between the α/β-domain and the helical domains, which is large enough to accommodate an 8-HDF but has no space for an MTHF at the corresponding position. No significant electron density for the second cofactor was found. However, in comparison with the 8-HDF-binding site in *A. nidulans* photolyase, the amino acid residues interacting with 8-HDF were found at almost the same position in the *T. thermophilus* enzyme. Based on these findings, Komori and coworkers suggested that *T. thermophilus* photolyase can be of 8-HDF-type.

In all three photolyases, the flavin cofactor lies deeply buried in the center of the helical domain with direct access to solvent limited to a cavity leading from the edge of the adenine moiety of FAD to the enzyme surface. A band of positive electrostatic potential, suitable for contact with the negatively charged phosphate backbone of the damaged DNA strand, runs along the outside of the protein around the cavity entrance. One side of the cavity consists of hydrophobic amino acid residues, and the other side has polar groups. This asymmetry is also a property of the CPD site of damaged DNA, in which the CPD's cyclobutane ring is hydrophobic and the opposite edges of the thymine bases have nitrogens and oxygens capable of forming hydrogen bonds. The cavity opening is wide enough to accommodate a CPD provided that it is extruded from the duplex [109]. Such base-flipping out of double-helical DNA has been observed in many DNA-repair systems, in which the enzymes need to approach the DNA bases in order to perform a reaction on them [112].

4. Substrate binding

Photolyases must be extremely efficient at distinguishing pyrimidine dimers in DNA from of a large excess of non-dimerized pyrimidine doublets as the number of photolyase molecules per cell is rather small: *E. coli* contains approximately 10–20 molecules of CPD photolyase per cell [113] and yeast 75–300 [114,115]. The flavin cofactor, but not the second chromophore, plays an important role in substrate binding: apophotolyase without the FAD is unable to bind to DNA. Once the apoenzyme is reconstituted with FAD, its specific affinity to UV-induced DNA lesions is restored [116]. Substrate binding is independent of the redox state of the flavin [116,117]. Photolyases are structure-specific DNA-binding proteins, whose specificity in recognizing pyrimidine dimers is determined by the configuration of the DNA phosphodiester backbone at the damage site and/or the structure of the DNA lesion itself, in contrast to sequence-specific DNA-binding proteins which rely on hydrogen-bond donors and acceptors in the grooves of the duplex [118–120].

CPD substrate binding to CPD photolyase occurs with comparable affinity to double-stranded and single-stranded DNA [120,121] with an association-rate constant in the 10^6 M^{-1} s^{-1} range [122]. Studies on the *E. coli* and *S. cerevisiae* CPD photolyase enzymes have shown that the equilibrium association constant for *cis–syn* CPDs in DNA (specific binding) is 2.6×10^8 to 2.2×10^9 M^{-1} [119,123], and 3.7×10^9 M^{-1} [124], respectively, whereas the association constant for the undamaged DNA (nonspecific binding) is more than four orders of magnitude lower.

The affinity of CPD photolyase to the *trans–syn* configured damage is identical or very close to the enzyme's affinity to undamaged DNA (association constant in the 10^4 to 10^5 M^{-1} range). Once bound, however, the *trans–syn* CPD is repaired with photochemical efficiency comparable to that of the *cis–syn* isomer [125]. The enzyme furthermore binds to UV-dimerized thymine-uracil (T◇U) and cytosine–cytosine (C◇C) bases, as well as to uracil–uracil (U◇U) bases in DNA and RNA [126].

Detailed structural information on photolyase-to-substrate binding at a molecular level is still not available due to the lack of high-quality co-crystals comprising the photolyase holoenzyme bound to a strand of UV-damaged DNA. Precise information on the distance between the CPD and the redox-active flavin cofactor, however, is essential for a thorough understanding of the mechanistic details of photoinduced DNA repair. Therefore, extensive biochemical and biophysical studies have been carried out to unravel the mode of substrate docking, binding sites, and docking geometries.

Atomic force microscopy has been used by van Noort et al. [127] to visualize the conformation of DNA when *A. nidulans* CPD photolyase is bound to intact and damaged DNA. In the former, no bending of DNA was found, whereas in the latter, average DNA bending angles of about 36° have been observed. This may include a slight intrinsic bend at the lesion site, but it is likely to be induced mainly by the protein. The standard deviation of the bending-angle distribution has been used to obtain information on the

flexibility of DNA characterized by its persistence length. While in nonspecific complexes protein-bound DNA was found to be more rigid than naked DNA, an increased flexibility was observed in specific complexes. This result was accounted for by the flipping-out model, with the CPD flipped out of the DNA helix, leaving behind the two adenine bases on the opposite strand that are then no longer hydrogen-bonded. Such unpaired bases in double-helical DNA are expected to increase DNA flexibility similar to base gaps.

The contact sites on UV-damaged DNA have been determined by footprinting studies with various class-I and class-II CPD photolyases [97,118,128]. The enzyme establishes intimate contact with a region comprising six to eight base pairs disposed around the dimer in the DNA. Backbone contacts are apparent at the first phosphate at the 5′-side of the dimer, and three to four phosphates at the 3′-side of the dimer on the dimer-containing strand, as well as at a single phosphate on the non-dimer strand located across the minor groove from the 5′- and intradimer phosphate.

The amino acid residues at the enzyme surface of yeast photolyase that contribute to high-affinity substrate binding and binding specificity have been identified by chemical modification and site-directed mutagenesis [124]. K517 was found to play an important role in binding of photolyase to DNA. In all microbial photolyases sequenced so far, the residue at the equivalent position is either lysine or arginine, suggesting a strict functional requirement for a positive charge at this position. Alanine substitutions of the conserved amino acids R507, K463 and W387 reduced both the overall affinity for substrate and substrate discrimination. The equivalent residues of K517 and R507 in *E. coli* photolyase, K407 and R397, are located within the band of positive electrostatic potential that runs across the surface of the enzyme near the putative substrate-binding site [109]. W277 (the *E. coli* equivalent of W387 in yeast photolyase) lies at the rim of the cavity. It contributes to substrate specificity either by van der Waals or π-stacking interactions as has been demonstrated by site-specific mutagenesis [123].

Alanine substitution mutations in yeast photolyase at conserved sites K330, E384 and F494 within the cavity also slightly reduced substrate binding and discrimination [129]. Because these residues lie too deeply buried inside the cavity to interact with normal B-DNA, the only explanation for these results is that the substrate undergoes a dramatic structural alteration, such as dimer flipping, that places these amino acids within interacting distance to the CPD. These findings have therefore been interpreted to support the dinucleotide-flip model.

More direct evidence for CPD base flipping by photolyase was presented by Christine et al. [130] from a recent examination of fluorescence yields in DNA substrates in which the adenine base opposing the 3′-thymine of a thymine doublet has been replaced by the adenine analog 2-aminopurine, a fluorescent reporter of helical structure. Due to base stacking facilitated by favorable Watson–Crick base pairs in annealed double-stranded DNA, the fluorescence of 2-aminopurine is significantly quenched. This is regardless of whether 2-aminopurine is hydrogen-bonded to a non-dimerized or to a CPD-dimerized thymine in the complementary strand. The 2-aminopurine's fluorescence is almost completely restored to its value in single-stranded DNA when the CPD-containing duplex is bound to photolyase. Such a large change in fluorescence yield indicates that by interaction of UV-damaged DNA with photolyase, a severe distortion of the local helical structure around the 2-aminopurine base has occurred. This is consistent with base flipping of the lesion into the protein-binding cavity with a concomitant de-stacking of the opposing complementary 2-aminopurine nucleotide.

Support for the model was also obtained from recent molecular dynamics simulations using the AMBER force field. Sanders and Wiest [131] examined three models for *E. coli* CPD photolyase enzyme–substrate complexes: photolyase docked to (a) a CPD dinucleotide, (b) a CPD-containing nine-nucleotide DNA strand, and (c) CPD-containing double-stranded dodecamer with and without CPD flipping. Interactions of the deoxyribophosphate backbone on the 5′-side of the CPD with R342 and R397 and on the 3′-side with K154 become apparent. The CPD in the active site is in contact with the two tryptophans W277 and W384, which create a fairly hydrophobic binding pocket for the CPD. Interestingly, in all three models no close contact between the CPD and the flavin cofactor of the holoenzyme is established. Distances between the CPD and the isoalloxazine ring of FAD of 15 and 12 Å were predicted for the non-flipped and the flipped-out configurations of the lesion, respectively. Even for the dinucleotide CPD, which is obviously the least restricted lesion regarding flexibility mediated by the bulky phosphate backbone, a minimum distance between C(5) on the 3′-base of the CPD and the ribose chain of FAD larger than 6 Å was calculated.

Large CPD-to-FAD cofactor distances have also been predicted from a second molecular dynamics simulation in which the docking of photolyase to "bare" (with both pyrimidine bases linked only by the cyclobutane ring) and "dressed" (with the pyrimidine bases also linked by the deoxyribose phosphate backbone) pyrimidine dimers has been examined by Hahn et al. [132]. In this work, also the shape of the substrate-binding pocket in the enzyme has been probed. A bottleneck region was identified at about 8 to 12 Å above the bottom of the cavity where the FAD is situated, in the direction leading toward the surface of the enzyme.

In contrast to the aforementioned model calculations, Antony et al. [133] have calculated a very short CPD-to-FAD distance of less than 3 Å in a third molecular dynamics study. In the average configuration, the docked thymine dimer is sitting deep in the enzyme cavity, approaching the isoalloxazine ring of FAD from the "open" side between the ribityl chain and the methyl group at C(8). With a distance

of ≈ 2.5 Å between the hydrogen atoms on the FAD's C(8α) methyl group and those on the methyl group of the 3′-thymine in the CPD, a significant deformation of the damaged strand in the DNA is expected.

In a further modeling study by Vande Berg and Sancar [129], docking of a CPD to *S. cerevisiae* photolyase was examined. Beginning with the structure of the putative DNA binding domain of the *E. coli* enzyme as a starting geometry, the structure of the equivalent region in the yeast enzyme was modeled. Neither coordinates nor distances were presented; however, shorter rather than longer CPD-to-FAD distances were preferred.

Recently, electron paramagnetic resonance (EPR) and electron-nuclear double resonance (ENDOR) were used by Weber et al. [134] to probe docking of a CPD to *E. coli* photolyase utilizing the FAD cofactor in its neutral radical form as a naturally occurring electron-spin probe. Compared to the flavin proton hyperfine-line positions in the ENDOR spectrum of free photolyase in frozen solution, small shifts were observed when UV-damaged DNA containing one or more CPDs is bound to the enzyme. The changes of the hyperfine couplings upon docking of substrate are too small to be consistent with a distance of less than 6 Å between the CPD and the FAD's isoalloxazine ring, on which the unpaired electron spin is located. Therefore, the EPR/ENDOR results support those model calculations that predict a large distance between the flavin and the CPD [131,132]. The observed subtle shifts of the isotropic proton hyperfine-coupling constants of the isoalloxazine moiety could be rationalized in terms of changing polarity of the cofactor environment once the substrate is docked to the enzyme. The trends observed are consistent with the substrate-binding pocket becoming less polar because of the displacement of water molecules upon substrate binding.

To yield information on the CPD-to-FAD distance in photolyase, MacFarlane VI and Stanley [135] used an electrochromic-shift model to quantitatively describe a spectral blue shift of the optical absorption bands of the flavin cofactor (in the fully oxidized redox state, FAD^{ox}) observed upon binding of the enzyme to a polynucleotide single-stranded CPD substrate [136]. No shift was observed for a dinucleotide CPD, suggesting that there are significant differences in the binding geometry of dinucleotide versus polynucleotide dimer lesions (see also Ref. [137]). Under the assumption that the band shifts arise from a strong dipolar electric field in the enzyme cavity due to the permanent dipole moment of the two coplanar thymine bases in the CPD, the authors obtained the binding distance from the CPD to the FAD^{ox} in photolyase, however, as a function of the effective dielectric constant of the protein. Assuming a realistic range of dielectric constants of $\varepsilon = 2.6–10$, the analysis yielded a distance range between 5.5 and 8 Å, implying that substrate and flavin cofactor are not in van der Waals contact. Using transient absorption spectroscopy, it was furthermore demonstrated that substrate binding does not significantly alter the structure of the protein around the FAD binding site. This observation is consistent with findings from EPR and ENDOR that also revealed only minor changes of the electronic structure of the flavin upon docking of the enzyme to photodamaged DNA [134].

An electrochromic shift of the flavin cofactor's optical absorption bands due to the presence of the dipolar thymidine-dimer substrate, previously reported for FAD^{ox} [135,136], has recently also been observed by Schelvis et al. [138] in the absorption spectrum of the flavin-cofactor in the semiquinone redox state, $FADH^{\bullet}$. However, because the difference dipole moments for transitions from the $FADH^{\bullet}$ ground state to excited singlet states are not known, CPD-to-FAD distance and orientation parameters could not be extracted from these experiments.

Using resonance Raman spectroscopy, the interaction between photolyase and UV-damaged DNA has been further investigated [138]. Changes in Raman intensities could be largely explained by changes in the Raman excitation profiles due to the electrochromic shift. The observed subtle frequency shifts of some $FADH^{\bullet}$ vibrations on binding of substrate to photolyase were proposed to arise primarily from small changes in the hydrogen-bonding interaction between $FADH^{\bullet}$ and its protein environment. Interestingly, when the resonance Raman spectrum of *E. coli* CPD photolyase containing the light-harvesting MTHF chromophore was compared with the one obtained previously by Murgida et al. [139] from a photolyase mutant (E109A) lacking the ability to bind MTHF, slight differences were revealed that suggest that the second chromophore may play a structural role in stabilizing the protein environment of the FAD cofactor.

As mentioned before, no crystal structure of the enzyme–substrate complex is available to date, but a recent X-ray structure of *T. thermophilus* photolyase complexed with thymine was published by Komori et al. [111]. The single thymine was shown to reside in the putative substrate cavity, making van der Waals contact with the isoalloxazine ring of FAD. A resonance Raman investigation of *E. coli* photolyase supplemented with a large excess of thymine, on the other hand, did not reveal any interaction between flavin and thymine [138]. This is most likely due to the very low affinity that thymine has for the photolyase substrate's cavity, although the possibility that thymine binding does not perturb the protein conformation and the flavin binding could not be ruled out. In any case, while one thymine molecule is clearly not a substrate, it can be thought of as a partial product of the repair reaction. As the inner part of the cavity is probably too small for two thymine bases, a CPD might therefore be located at the outer side at a larger distance to the redox-active moiety of FAD.

5. Reaction mechanism of photoreactivation

The reaction mechanism of photoreactivation of UV-damaged DNA catalyzed by photolyases and the role of

the two chromophores in this process have been studied quite extensively. The present commonly accepted model for the individual steps of the enzymatic reaction in the CPD-repairing protein is given in Fig. 4A. Nevertheless, one should keep in mind that some important details in the hypothetic pathway of catalytic DNA repair have not yet been definitely established and therefore deserve further examination [46].

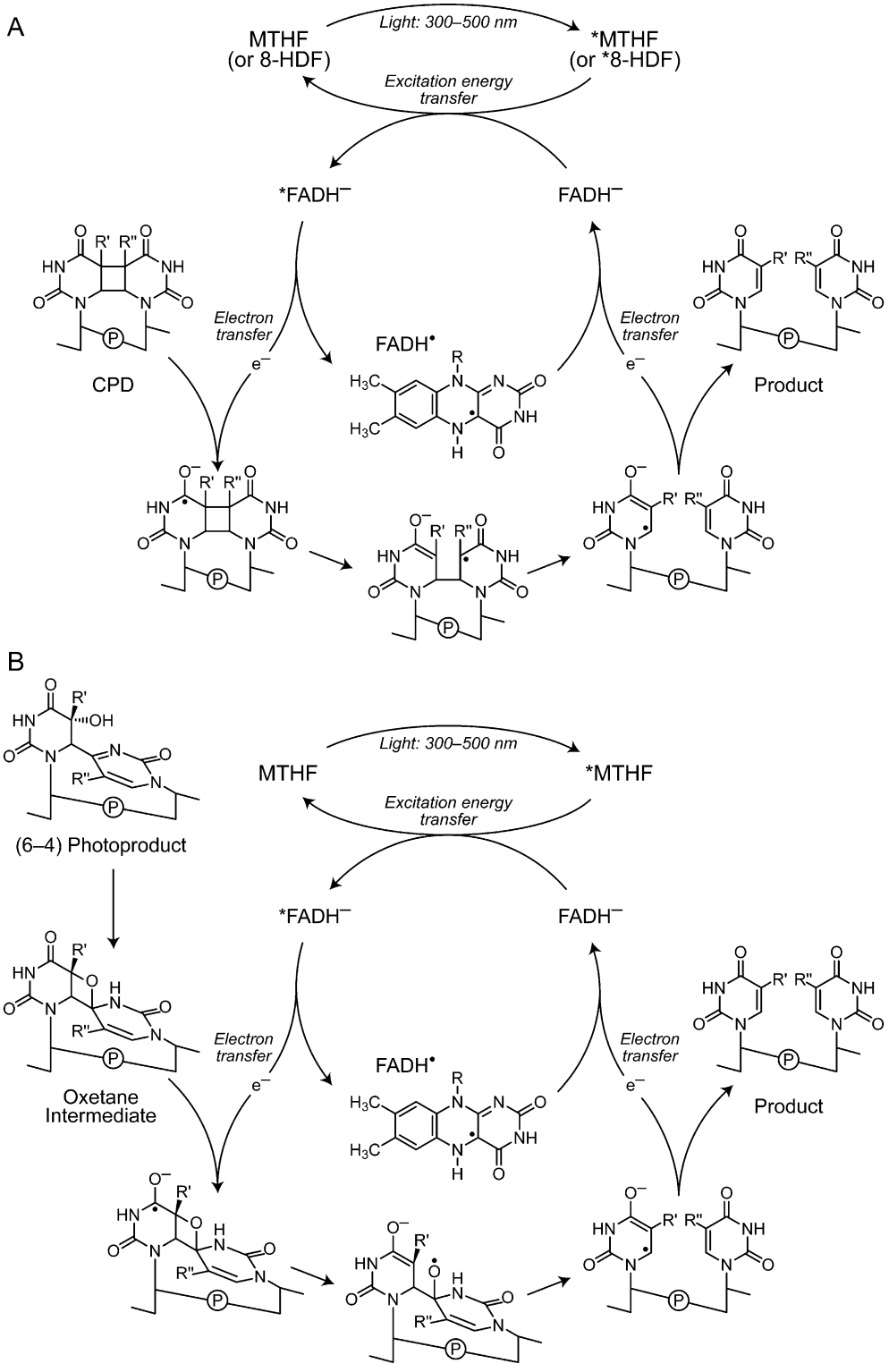

Fig. 4. The putative reaction mechanism of CPDs by CPD photolyase (A) and (6–4)PPs by (6–4) photolyase (B). R is defined in Fig. 2. R′ and R″ are either CH_3 in thymine or H in uracil.

5.1. Energy transfer between the light-harvesting chromophore and the flavin cofactor

The flavin cofactor plays the essential role in catalysis. Even though the enzyme may be stabilized with the FAD in all three redox states (see Fig. 2), only the one with fully reduced $FADH^-$ is catalytically active both *in vitro* [117,140,141] and in vivo [142]. The presence of the second chromophore is not required for DNA repair [143,144]. Its sole function is to gather light by absorption in the regions of near-UV and visible wavelengths (where $FADH^-$ absorbs very weakly) and transfer the excitation energy to $FADH^-$ to yield the excited singlet state $*FADH^-$ [120,136,143,145]. Both excitations are singlet $\pi-\pi^*$ transitions from the highest occupied molecular orbital (HOMO) to the lowest unoccupied molecular orbital (LUMO). In the absence of a second chromophore, $*FADH^-$ can also be generated by direct photoexcitation of $FADH^-$ [146]. Kim et al. [147] have determined the fluorescence lifetimes of the second antenna chromophores in flavin-deficient *E. coli* and *A. nidulans* apophotolyase. Fluorescence decays of 354 ps at 470 nm [147] and 2 ns at 435 nm [148] have been measured for enzyme-bound MTHF and 8-HDF, respectively. In the presence of $FADH^-$, these lifetimes are reduced to 134 and 50 ps due to energy transfer from the excited singlet state of the second chromophore to $FADH^-$. Rate constants of 4.6×10^9 and 1.9×10^{10} s^{-1} as well as quantum yields of 0.62 and 0.98 have been determined for this process in *E. coli* [147] and *A. nidulans* [148] photolyase, respectively. Concomitant with the decay of the transient absorption signal of the first excited singlet state of MTHF, the appearance of a new band at 500–600 nm, previously assigned to the first excited singlet state of enzyme-bound $FADH^-$ [146], was detected by picosecond flash photolysis [147].

The mechanism of energy transfer between the cofactors is believed to be of Förster type via long-range dipole–dipole interaction between $FADH^-$ and either MTHF or 8-HDF. In principle, an analysis of the fluorescence data utilizing the formalism derived by Förster yields information on the distance between the interacting chromophores. For the *A. nidulans* photolyase, a spatial separation of 15 Å was predicted based on this theory, long before the X-ray structure of the enzyme had been solved [110]. For the *E. coli* photolyase, an $FADH^-$-to-MTHF distance of 22 Å was obtained which is larger than that revealed from the crystal structure (16.4 Å) [109]. One reason for this discrepancy might be that the orientation of the transition dipoles is not random, as was assumed for the analysis of the fluorescence data. Another explanation could be that there is a distribution of differently bound MTHF in the *E. coli* enzyme, thus yielding an apparent distance that is larger than the one obtained if MTHF were only located in its original binding-site at the enzyme surface. MTHF is known to be less tightly associated with the protein resulting in a partial loss of this chromophore during enzyme purification. To obtain preparations with stoichiometric amounts of MTHF, it is therefore often supplemented [149, 150].

5.2. Electron transfer from the flavin cofactor to the CPD lesion

In the excited singlet state, $*FADH^-$, the flavin transfers an electron to the CPD lesion to generate a semiquinone flavin radical ($FADH^\bullet$) and a CPD anion radical that subsequently undergoes cycloreversion. Okamura et al. [146] have obtained direct evidence for photoinduced electron transfer in the catalytic pathway by observation of a radical intermediate in a picosecond laser-flash photolysis experiment on MTHF-deficient *E. coli* CPD photolyase. The broad absorption band appearing in the 500–900-nm region, which has been assigned to the first excited singlet state of $FADH^-$, decays much faster in the presence of U◇U-containing substrate than it does in the absence of substrate (160 ps versus 1.4 ns). This observation is consistent with previous reports by Jordan and Jorns [151] who showed selective quenching of the $FADH^-$ fluorescence in an enzyme–substrate complex. From the lifetimes of the excited state, $*FADH^-$, the rate of forward electron transfer from $FADH^-$ to the CPD (in either a dimeric or a 15-mer oligothymidine substrate), $k_{FET} = 5.5 \times 10^9$ s^{-1}, and the quantum yield, $\Phi_{FET} = 0.89$, have been determined by Kim et al. [147] using time-correlated single-photon counting. Analogous experiments on the *A. nidulans* enzyme have been carried out and yielded $k_{FET} = 6.5 \times 10^9$ s^{-1} and $\Phi_{FET} = 0.92$ [148]. Later UV transient absorption experiments (265-nm probe wavelength) with this enzyme bound to a pentameric oligothymidine substrate, however, revealed a considerably higher electron-transfer rate ($k_{FET} = 3 \times 10^{10}$ s^{-1}) [152]. The corresponding much faster electron-transfer lifetime suggests that the FAD-to-CPD distance might be shorter than previously thought.

In the transient absorption spectra of MTHF-deficient *E. coli* CPD photolyase bound to a U◇U substrate, a new band at around 400 nm that appeared with increasing delay time after the excitation pulse has been observed by Okamura et al. [146]. It was suggested that this transient represents an essential intermediate in the reaction pathway leading to CPD splitting. However, due to the lack of reference spectra, it was not possible to assign the transient to either a flavin radical or a U◇U radical. In a subsequent study, Kim et al. [153] reexamined these findings, again by laser-flash photolysis, however, using different photodimer substrates (namely U◇T and T◇T). The 400-nm species previously observed with U◇U was also observed with U◇T, however, with peak-absorbance at 420 nm, but not with T◇T. The decay time of the transient was close to the instrumental time response of the spectrometer but was nevertheless estimated to be in the 0.5 to 2-ns range. The lack of the 400–420-nm signal with T◇T was assumed to be due to an even shorter lifetime of this transient or due to a shift of the absorbance of the transient outside the spectral

region probed. Based on their observations, Kim and coworkers concluded that the transient absorbance arises from the substrate rather than the flavin.

Using transient absorption spectroscopy with picosecond time resolution, Langenbacher et al. [154] have studied the lifetime of the first excited singlet state of $FADH^-$ at different temperatures and the acceleration of the $*FADH^-$ decay by electron transfer in various enzyme–substrate complexes. In MTHF-deficient *E. coli* photolyase without substrate, $*FADH^-$ decays with a time constant of about 1.8 ns at 275 K and 7.5 ns at 90 K. In the presence of substrate, the decay is more than 10 times faster (e.g., 110 ps in an enzyme–T◇T complex at 275 K) and depends on the nature of the substrate. This substrate dependence is even more pronounced at low temperatures. At 90 K, $*FADH^-$ decays fastest when photolyase is complexed with U◇T (130 ± 30 ps), followed by U◇U (170 ± 80 ps), T◇T (350 ± 60 ps) and T◇U (510 ± 90 ps). From these findings it was suggested that the T◇U substrate docks with photolyase in a less favorable orientation than does U◇T. Such a variation of the $FADH^-$-to-substrate distance would be consistent with steric hindrance of the methyl group of thymine when in 5′- rather than 3′-position of the CPD and explain the faster rates for U◇U and U◇T. The temperature dependence of the quantum yield of dimer repair was analyzed under the assumption that back electron transfer is temperature-independent and that dimer splitting is a thermally activated process. This yielded an activation energy of 450 ± 100 and 450 ± 200 meV for dimer splitting of U◇T and U◇U, respectively. Such an energy barrier is easily compensated at ambient temperature. Therefore, the whole photoreactivation process has been regarded as a "photon powered" reaction [33].

Further evidence for a radical intermediate during photolysis of a CPD comes from time-resolved EPR [155]. Short-lived EPR transients have been detected at different magnetic-field positions within the spectral range where the $FADH^\bullet$ resonances are typically observed. The presented kinetic traces rose and decayed rapidly with the time constant of the EPR spectrometer (35 μs). No EPR spectrum of the transient species was reported. Tentatively, the transients were assigned to the final radical-pair state $FADH^\bullet\cdots TT^{\bullet\,-}$ rather than the initial state $FADH^\bullet\cdots T◇T^{\bullet\,-}$. In the light of more recent EPR data published by Gindt et al. [156], however, this assignment appears questionable (see also below) and therefore requires verification by EPR with high time resolution in the nanosecond regime.

Rustandi and Jorns [157] used light-modulation EPR at 4 K to detect paramagnetic intermediates in the course of CPD repair. Splitting of the thymine dimer does not occur at this temperature and, therefore, a light-initiated flavin/substrate radical pair, $FADH^\bullet\cdots T◇T^{\bullet\,-}$, can only undergo back electron transfer which might, in principle, occur on a longer time scale. Indeed, a weak first-derivative EPR signal has been detected using modulation of the excitation-light intensity (modulation frequency, 500 Hz). Upon signal integration, a spin-polarized EPR spectrum with an emission/enhanced-absorption polarization pattern was obtained, as is typical for a doublet-pair species generated in a radical-pair mechanism with a singlet-state precursor. Unfortunately, the light-modulation EPR method does not reveal the lifetime of the transient paramagnetic species observed. Therefore, no information on the rate of forward and backward electron transfer was obtained.

In a theoretical examination of electron transfer between $FADH^-$ and the CPD in a computer-modeled enzyme–substrate complex (see also above), Antony et al. [133] calculated the electron-transfer matrix element for the coupling between the LUMOs[3] of electron donor and acceptor. The root-mean-square transfer matrix element along the dynamic trajectory of a molecular dynamics simulation was found to be 6 cm^{-1} with a variance of 5 cm^{-1} for a T◇T substrate. Slightly larger values of 7 cm^{-1} with variances of 5, 5, and 6 cm^{-1} were reported for T◇U, U◇T, and U◇U substrates, respectively. The calculations predicted that despite the short distance of less than 3 Å assumed between $FADH^-$ and the CPD, the electron-transfer mechanism is not direct, but indirect with the adenine moiety of $FADH^-$ acting as an intermediate. The proposed superexchange-type mechanism utilizes the unusual conformation of the flavin cofactor specific for photolyases, in which the isoalloxazine ring and the adenine ring are in close proximity [109–111,158] leading to a certain overlap of their π-systems. The strong coupling of the donor and acceptor states with the same intermediate electronic states of the adenine causes an effective coupling between the CPD and $FADH^-$ without the necessity for direct orbital overlap. The pathway of electron transfer between these moieties has been calculated by Medvedev and Stuchebrukhov [159] using the method of interatomic tunneling currents. Initially, the electron (probability) density is predicted to be delocalized mostly on the rings I and II (see Fig. 2) of the FAD's isoalloxazine moiety. The main tunneling path leads via C(1′), H(1′) in the ribityl side chain to N(1), C(6) and 6-NH_2 on the adenine ring, and from there to the C(4)=O(4) carbonyl groups as the main acceptor sites on both thymine bases of the CPD.

Results from EPR and ENDOR experiments by which the extent of delocalization of the unpaired electron spin over the $FADH^\bullet$ cofactor's isoalloxazine moiety is probed support the superexchange model of photolyase-mediated CPD repair [160,161]. The singly occupied HOMO (=SOMO) of $FADH^\bullet$ constitutes the electron acceptor site in back electron transfer from either $T◇T^{\bullet\,-}$ or the repaired $TT^{\bullet\,-}$. Proton hyperfine couplings, as determined by EPR and ENDOR spectroscopy, provide an indirect probe of the electron-density distribution in this frontier orbital, as spin

[3] The LUMO is taken as representative of the electronic distribution of the donor as an electron of the HOMO is promoted to the LUMO preceding to electron transfer.

density at the protons usually arises from spin polarization and/or hyperconjugation with the main π-electron system situated on the carbons and nitrogens. Compared to other flavoenzymes that catalyze one-electron transfer reactions [87], the unpaired electron-spin density in $FADH^{\bullet}$ of *E. coli* CPD photolyase is more confined to the rings I and II (see Fig. 2) of the isoalloxazine moiety whereas the electron-spin density on the outer ring III is very low. This is manifested by the smallest detected isotropic proton hyperfine coupling of an 8-methyl group in a neutral flavin radical in flavoenzymes so far [160].

The immediate protein environment plays an important role in fine-tuning the electronic structure of the flavin for highly optimized electron transfer (see Fig. 5C) [161]. The fact that the unpaired electron-spin density and approximately also the electron density on the flavin's benzene ring is small, even though this part of the FAD's isoalloxazine moiety is in the direction of the CPD lesion, is a clear indication that the electron transfer between the isoalloxazine ring and the dimer is not direct. The large amplitudes of the SOMO on the central pyrazine and the pyrimidine rings increase orbital overlap between the π-systems of the isoalloxazine and the adenine moieties of FAD (see Fig. 5B). It was therefore assumed that the adenine bridges the gap between FAD and the CPD. Whether the electron transfer between the CPD and the adenine of FAD is direct or sequential through redox-active amino acids such as tryptophan as intermediates is a question that awaits clari-

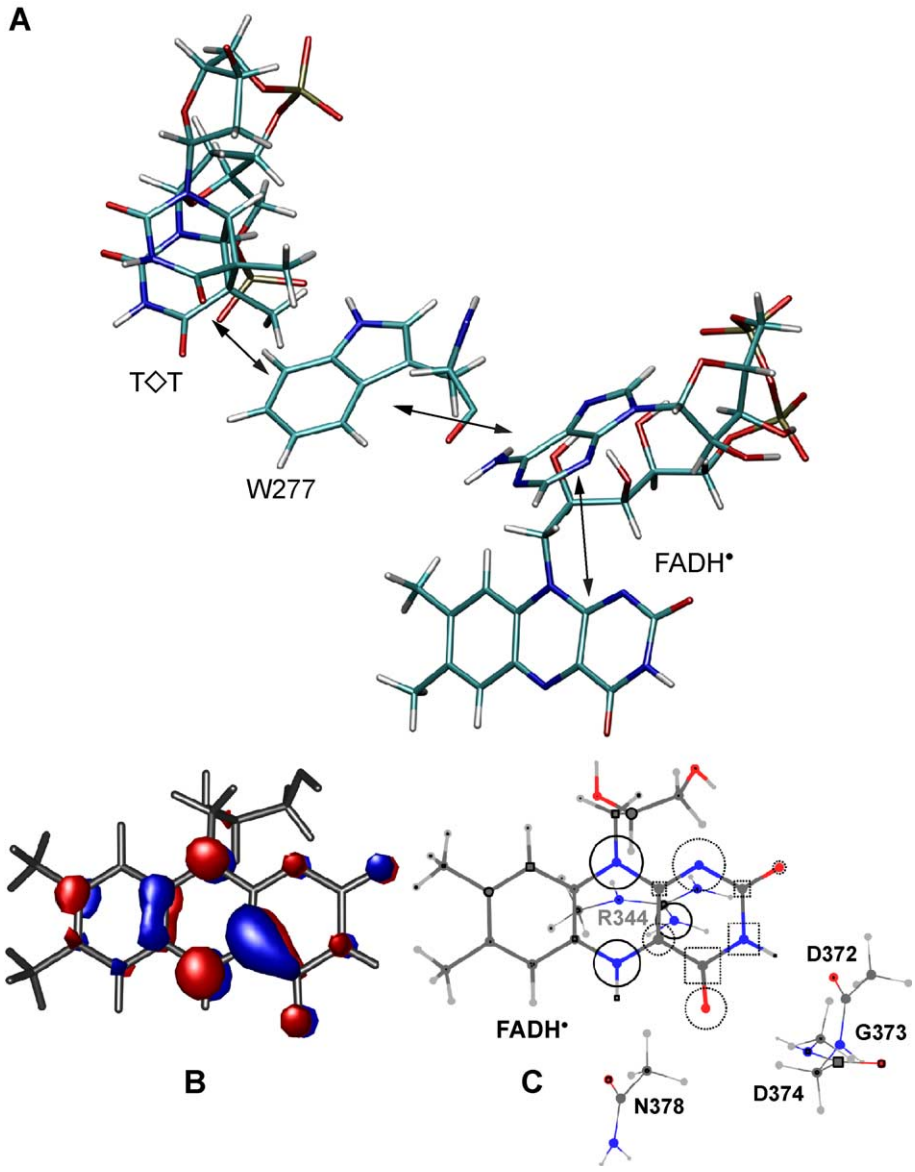

Fig. 5. (A) Proposed electron-transfer pathway between the isoalloxazine ring of FAD and the T◇T dimer. (B) The singly occupied molecular orbital (SOMO) of $FADH^{\bullet}$ calculated using density-functional theory [161]. (C) Influence of the amino acid residues R344, D372, G373, D374, and N378 on the s-spin density of the SOMO of $FADH^{\bullet}$. Circles and squares represent positive and negative s-spin density, respectively. Increasing absolute spin density at the nuclei is depicted by full symbols, whereas a decrease of spin density is shown by dotted-line symbols. For further details see Ref. [161].

fication from a co-crystal structure comprising the photolyase enzyme bound to substrate. W277 could be one candidate as intermediate electron acceptor (see Fig. 5A).

W277 has also been shown to be capable of directly repairing CPDs (with a quantum yield of 0.56) when photoexcited with short-wavelength UV light of 280 nm [162]. The absolute action spectrum, tryptophan fluorescence and fluorescence quenching by substrate combined with results from site-directed mutagenesis suggested that W277 alone functions as the photosensitizer during this repair. In support of this postulate, W277 is close to the putative substrate-binding site in the crystal structure. However, taking into account the low flux in sunlight at wavelengths below 300 nm, the contribution of this W277-mediated photoreversal of pyrimidine dimers by photolyase is less than 0.01% compared to repair involving the MTHF and $FADH^-$ cofactors.

5.3. Splitting of the CPD

Little information is available on the mechanistic details of enzymatic cyclobutane-ring opening in photodamaged DNA bound to photolyase. What is known comes mostly either from model studies, such as pulse-radiolysis experiments in the presence of photosensitizers (see, e.g., Refs. [34,163]), or from quantum-chemical calculations at various levels of theory [164–168]. However, most of the computational studies were performed for CPDs in the gas phase, and their applicability to reactions in solution or with the enzyme is not clear. The consensus to date is that in a CPD radical anion, such as $T\diamond T^{\bullet -}$ or $U\diamond U^{\bullet -}$, the C(5)–C(5′) σ-bond breaks first with small activation energy, leading to the formation of an intermediate (see Fig. 4) [164–167]. This is followed by the cleavage of the C(6)–C(6′) σ-bond. An activation barrier of 611 meV and an endothermicity of 572 meV for this step have been predicted from an unrestricted HF computation [167]. Using density-functional theory methods, cleavage of the C(6)–C(6′) σ-bond was found to be slightly exothermic (-104 meV) with a 99-meV energy barrier [166]. However, when water molecules were allowed to hydrogen-bond to a U◇U dimer, the anionic cycloreversion became downhill by 663 meV and essentially barrierless [167].

Recently, MacFarlane IV and Stanley [152] have used subpicosecond UV transient absorption spectroscopy to trace the repair kinetics of *A. nidulans* photolyase bound to either dimeric or pentameric oligothymidine substrate. Different to previous flash-photolysis experiments, they have monitored the UV spectral region at 265 nm because the breaking of the CPD's cyclobutane ring leads to the reformation of the double bonds C(5)=C(6) and C(5′)=C(6′) of the adjacent thymines which both strongly absorb in this range. Their results suggest that the cyclobutane-ring opening proceeds sequentially rather than in a concerted fashion. The breaking of the first σ-bond was found to be nearly activation-less and takes place within approximately 60 ps. A slower increase of the 265-nm absorption up to 1.5 ns was assigned to the re-formation of the second double bond. This second step has a significant energy barrier. Pronounced differences in the repair kinetics have been observed when substrates of different length were examined, e.g., dimeric versus pentameric oligothymidines. The findings are consistent with previous observations that dimeric T◇T substrates assume a different geometry when bound to photolyase compared to longer oligomers [137].

Interestingly, from their optical experiments, MacFarlane IV and Stanley [152] conclude that the flavin cofactor remains in the semiquinone state ($FADH^\bullet$) after repair rather than being re-reduced to $FADH^-$ by back electron transfer from $TT^{\bullet -}$. No $FADH^\bullet$ buildup was observed in the *A. nidulans* enzyme without substrate. If these preliminary findings prove to be correct, then the excess electron on the thymine bases would have to be donated to electron acceptors different from $FADH^\bullet$, which are abundant in a cell. In this case, the $FADH^\bullet \rightarrow FADH^-$ reactivation would not occur within the repair process but would require an additional photoinduced electron-transfer process towards the flavin cofactor (see also below) as a prerequisite for further enzymatic activity. Accumulation of $FADH^\bullet$ in CPD repair has been reported previously, however, under high excitation intensities (>100 μJ/mm^2) regardless of whether substrate was present or not [154]. That $FADH^\bullet$ buildup was not observed in other repair studies was explained with the longer laser pulses utilized in previous experiments. If the excitation pulses were sufficiently long and intense so that two sequential electron-transfer processes (reductive T◇T-dimer cleavage and subsequent $FADH^\bullet$ photoreduction) are initiated with one single pulse, a photoreduction step leading to fully reduced $FADH^-$ could in principle immediately follow the repair reaction to complete the catalytic cycle. In this case, however, the overall quantum yield of CPD repair may not exceed 0.5. Hence, the results from time-resolved experiments as reported by MacFarlane IV and Stanley [152] are at odds with steady-state quantum-yield studies from other laboratories that gave repair quantum yields that range from 0.7 to 0.9 [117,120,169].

In earlier work, Kim and Rose [170] and Kim et al. [171] observed that in isotropic solution, reductive CPD splitting dramatically depends on the dielectric constant of the solvent. In nonpolar solvents the cleavage reaction is much more efficient than in polar solvents, reaching a maximum for the least polar solvent investigated. It has been suggested that this observation may be rationalized by the fact that back electron transfer from the dimer to the photosensitizer is slowed in nonpolar solvents as it pushes the reaction into the Marcus-inverted region, thus increasing the efficiency of the cleavage reaction. Likewise, in enzymatic DNA photorepair it may be that photolyases use their low-polarity active site (as observed in early optical studies but also recently using EPR and ENDOR [134,160]) to slow down back electron transfer from $T\diamond T^{\bullet -}$ to $FADH^\bullet$ and thereby to enhance the competitive splitting reaction.

6. Photoreduction of the flavin cofactor

A second photoreaction has been observed in photolyase, regardless of whether the enzyme is free in solution or complexed to the appropriate DNA lesion. The photoreaction is characteristic of enzyme with the flavin cofactor in the (inactive) neutral radical form, $FADH^{\bullet}$, or the (also inactive) fully oxidized redox state, FAD^{ox}. By absorption of light in the visible range, both $FADH^{\bullet}$ and FAD^{ox} undergo a photoreduction in the presence of reducing agents to yield the catalytically active $FADH^{-}$ form. This process has therefore been named photoactivation (not to confuse with photo*re*activation of DNA). Flavin photoreduction is not unique in the photolyase-protein family; the reaction, which is often conducted in the presence of EDTA, has been observed in a wide range of flavoproteins [172,173]. In early studies on photolyase-mediated DNA repair, the $FADH^{\bullet}$ form of the enzyme was falsely assumed to be catalytically active, but it was photoactivation that promoted the otherwise inactive $FADH^{\bullet}$ to the competent $FADH^{-}$ form.

Photoactivation in photolyases has been studied quite extensively [46,174]. Using nanosecond flash photolysis, an absorption peak at 510 nm at 4 μs after the excitation flash has been observed in enzyme that had the flavin initially in the $FADH^{\bullet}$ form. Based on this finding, it was proposed that the immediate electron donor in flavin photoactivation was a tryptophan residue which, following its photooxidation, was reduced by reducing agents in the medium [175]. By individual replacement of each one of the 15 tryptophan residues in *E. coli* CPD photolyase with phenylalanine using site-directed mutagenesis, W306 was identified as the terminal electron donor, because only the W306F mutant abolished photoreduction of $FADH^{\bullet}$ without affecting the excited-state properties of $FADH^{\bullet}$ or the substrate binding of the enzyme [176].

The early work on the involvement of tryptophans in photoactivation and photoreactivation has been reviewed in 1995 by Kim et al. [177]. Since then, biophysical examination of flavin-cofactor photoactivation has experienced a fruitful renaissance driven by the elucidation of the three-dimensional structures of the *E. coli* [109] and *A. nidulans* [110] photolyases. In the *E. coli* enzyme, W306 was found to be near the protein surface, however, more than 14 Å away from the flavin. Such a large distance excludes a direct or superexchange-mediated electron transfer on a picosecond time scale [178]. Therefore, two hypothetic pathways for the electron transfer between W306 and $FADH^{\bullet}$ have been proposed [109]. One is via two other tryptophans, W382 and W359, which are located between W306 and $FADH^{\bullet}$ (see Fig. 6). The other putative pathway involves the polypeptide chain between residues 358 and 366, and the side chain of F366. Subsequent studies have focused on the W382 ← W359 ← W306 pathway, mainly because these three residues are highly conserved throughout the photolyase family, including CPD photolyases of class I and class II as well as (6–4) photolyases (see also below). All three tryptophans are also found in cryptochromes [63,179], which share a high degree of protein sequence homology with photolyases but do not have DNA repair activity [53,55,180]. Therefore, studies on the electron transfer in

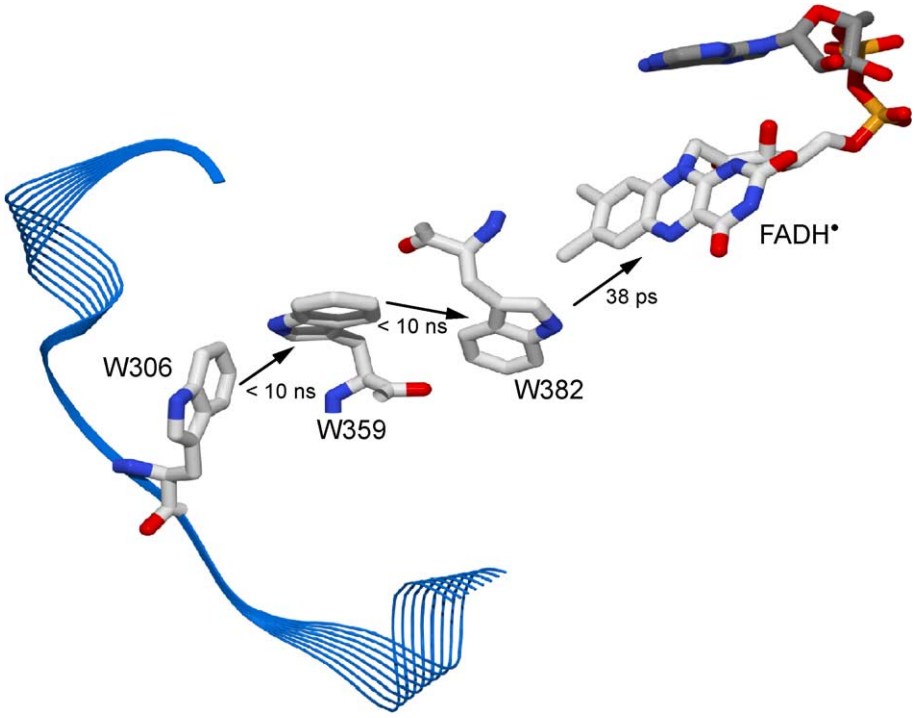

Fig. 6. Arrangement of the flavin cofactor and the tryptophan residues W382, W359, and W306 in *E. coli* CPD photolyase. The arrows indicate the direction of electron transfer in $FADH^{\bullet}$ photoactivation. The electron-transfer time constants for the individual steps were taken from Refs. [182,184].

photolyase photoactivation might be relevant for the examination of the reaction mechanism of the cryptochrome blue-light photoreceptors as well [181].

Very recently, W382 has been identified as the primary electron donor in $FADH^{\bullet}$ photoactivation of *E. coli* CPD photolyase [182]. This was achieved by a comparison of the decay of the transient absorption of photo-excited $FADH^{\bullet}$ in the spectral region from 650 to 820 nm using ultrafast pump/probe absorption spectroscopy applied to a wild-type photolyase and a mutant (W382F), where the tryptophan proximal to FAD has been replaced by phenylalanine. (Laser-flash induced absorption in this wavelength range has been previously assigned to $*FADH^{\bullet}$ [175,183].) In the mutant, F382 is assumed to adopt a geometry that is similar to that of W382 in the wild type. However, the F382's phenyl group is virtually unable to participate in electron transfer from W306 to the flavin. Probed at 500 and 700 nm, $FADH^{\bullet}$ excited-state lifetimes of 26 and 80 ps have been observed for the wild-type and the mutant photolyase, respectively. Under the assumption that the long decay represents the intrinsic lifetime for relaxation of $*FADH^{\bullet}$ to the ground state, which should be similar in the wild-type and the mutant, the electron-transfer rate constant for the primary electron-transfer step in photoactivation has been determined, $k = 2.6 \times 10^{10}\ s^{-1}$ [182]. The two subsequent electron-transfer steps from W359 to $W382^{\bullet +}$ (to yield $W359^{\bullet +}$ and W382), and from W306 to $W359^{\bullet +}$ to yield W359 and the radical cation $W306^{\bullet +}$ could not be resolved but were estimated to be completed within less than 10 ns (see Fig. 6) [184]. Within 300 ns, the surface-exposed $W306^{\bullet +}$ releases a proton to buffer molecules (when present at high concentrations) or water in the solvent rather than to a proton-accepting residue within the enzyme to yield a neutral $W306^{\bullet}$ radical:

$$
\begin{aligned}
&FADH^{\bullet}\ W382\ W359\ W306\\
&\xrightarrow{h\nu} *FADH^{\bullet}\ W382\ W359\ W306\\
&\rightarrow FADH^{-}\ W382^{\bullet +}\ W359\ W306\\
&\rightarrow FADH^{-}\ W382\ W359^{\bullet +}\ W306\\
&\rightarrow FADH^{-}\ W382\ W359\ W306^{\bullet +}\\
&\xrightarrow{-H^{+}} FADH^{-}\ W382\ W359\ W306^{\bullet}.
\end{aligned}
$$

The reaction mechanism proposed by Aubert et al. [184] is incompatible with a previously suggested reaction scheme, in which it was assumed that a long-lived quartet state of $FADH^{\bullet}$, formed by intersystem crossing from the initial excited doublet state $*FADH^{\bullet}$, abstracts an electron from W306 within 500 ns, and that the resulting $W306^{\bullet +}$ remains protonated [175,177,183,185]. The origin of the discrepancy was assumed to arise from optical excitation of redox forms other than $FADH^{\bullet}$, for example FAD^{ox}, when short-wavelength radiation sources were used.

A free-energy scheme for the radical transfer during photoactivation of *E. coli* photolyase was presented based on the excitation wavelength for $FADH^{\bullet} \rightarrow *FADH^{\bullet}$, and the midpoint potentials of the $FADH^{\bullet}/FADH^{-}$ (approximately − 0.4 V) and $W^{\bullet +}/W$ (approximately 1.1 V) couples. The initial electron transfer from W382 to $*FADH^{\bullet}$ was assumed to be downhill by approximately 500 meV while the two subsequent electron-transfer steps were estimated to be nearly isoenergetic. Deprotonation of $W306^{\bullet +}$ is driven by a substantial decrease in free energy of about 200 meV, thus stabilizing $W306^{\bullet}$ to prevent fast direct recombination [184].

Popovic et al. [186] computed the electrostatic free energies for the intermediating radical states from a solution of the Poisson–Boltzmann equation. They proposed that electron transfer from W359 to $W382^{\bullet +}$ is slightly endergonic (58 meV), whereas the electron transfer from the distal W306 to $W359^{\bullet +}$ is approximately 200 meV downhill in energy, thus funneling and stabilizing the radical state at W306. The $W306^{\bullet +}$ deprotonation was calculated to be 214 meV further downhill in energy.

Cheung et al. [187] described the results of a series of theoretical calculations of electron-transfer pathways between W306 and $*FADH^{\bullet}$ in *E. coli* CPD photolyase, using the method of interatomic tunneling currents. Their computations essentially confirmed the electron-transfer chain via the tryptophan residues that were originally proposed by Park et al. [109] from the crystal structure.

Flavin cofactor photoactivation has been studied also in *A. nidulans* CPD photolyase using transient absorption spectroscopy [188]. Different from the *E. coli* enzyme, a tyrosine residue was observed to be the final electron donor, reducing a tryptophan intermediate with a time constant of approximately 50 μs. The amino acid radicals were identified by their characteristic absorptions with maxima at 520 nm for $W^{\bullet}$ and 410 nm for $Y^{\bullet}$. In *A. nidulans* photolyase, however, the photooxidized $W^{\bullet}$ is only partially (approximately 40%) reduced by a tyrosine, whereas the majority (approximately 60%) of $W^{\bullet}$ is re-reduced by back electron transfer from the flavin. It is not clear to date whether this nonuniform behavior is caused by sample heterogeneity or results from competing reactions where the reduction of $W^{\bullet +}$ by tyrosine is energetically much less favorable than back electron transfer from the flavin. The tyrosyl radical can also recombine with $FADH^{-}$ but on a much slower time scale than $W^{\bullet}$ (76 versus 1 ms).

By taking advantage of a kinetic isotope effect, which is characterized by a prolongation of the tyrosine-radical lifetime in D_2O (198 ms) as compared to H_2O (76 ms), Aubert et al. [189] also succeeded to detect $Y^{\bullet}$ in *A. nidulans* photolyase by EPR spectroscopy (time resolution, approximately 10 ms). The tyrosine in photolyase was identified by comparison with EPR spectra from the Y_Z species of Mn-depleted plant photosystem II. From the *g*-value of the tyrosine resonance, $g \approx 2.005$, it was concluded that the tyrosine residue is deprotonated. To date, however, it is unclear which tyrosine residue participates in flavin

photoactivation of *A. nidulans* photolyase. If one assumes that W314 is the terminal tryptophan electron donor (W314 corresponds to W306 in *E. coli* photolyase), then the tyrosine closest to this residue is Y468 at an edge-to-edge distance of about 8.6 Å. There is, however, a further tryptophan, W309, bridging the gap between W314 and Y468. Y468 is at the surface of the enzyme and might therefore mediate electron transfer to reducing agents in the solvent. Its large distance to W314 would explain the slow formation time constant for electron transfer from Y468 to the tryptophan [186].

Gindt and coworkers reexamined earlier EPR observations [177,190,191] of a transient spin-polarized radical-pair signal detected upon photoreduction of *E. coli* CPD photolyase [156]. By measurement of the transient EPR signal amplitude as a function of the excitation wavelength and depending on the amplitude of the stationary (dark) EPR signal of $FADH^{\bullet}$ in different enzyme preparations, they concluded that the spin-polarized EPR spectra observed previously did not originate from photoactivation initiated by flavin-semiquinone photochemistry, but rather by photoactivation starting from the fully oxidized redox state of the flavin cofactor. They proposed that electron abstraction from a nearby tryptophan residue occurs via the triplet state of FAD^{ox} generated by intersystem crossing from an excited singlet state of FAD^{ox}. Evidence for the involvement of a flavin triplet state came from the disappearance of the spin-polarized EPR signal in the presence of potassium iodide, an effective triplet quencher (for flavins):

$$\begin{aligned} &FADH^{ox}\ W382\ W359\ W306 \\ &\quad \xrightarrow{h\nu} {}^{*}FADH^{ox}\ W382\ W359\ W306 \\ &\quad \xrightarrow{ISC} {}^{3}FADH^{ox}\ W382\ W359\ W306 \\ &\quad \rightarrow {}^{3}(FADH^{\bullet -}\ W382^{\bullet +})\ W359\ W306 \\ &\quad \rightarrow \cdots \rightarrow FADH^{\bullet}\ W382\ W359\ W306^{\bullet}. \end{aligned}$$

7. (6–4) Photolyase

7.1. Substrate binding

X. laevis and *D. melanogaster* (6–4) photolyases specifically bind to (6–4)PP-damaged double-stranded DNA with association constants of $2.1 \times 10^8\ M^{-1}$ [106] and $2 \times 10^9\ M^{-1}$ [107], respectively. (6–4) Photolyase also binds to single-stranded (6–4)PP-damaged DNA substrates and to DNA containing the Dewar isomer of the (6–4)PP. However, the affinities for these substrates are somewhat lower than that of (6–4)PP in double-stranded DNA [106,107].

7.2. Photoreactivation

Precise understanding of the mechanism of photorepair of (6–4)PPs by the enzyme (6–4) photolyase is scarce. No crystal structure is available to date. In the past, spectroscopic studies on the enzyme were often hampered by the limited quantities of enzyme available after overexpression. Furthermore, enzyme preparations frequently contained substoichiometric amounts of the two chromophores and were, therefore, not very well defined [99]. For these reasons, many conclusions on the catalytic cycle of (6–4)PP photoreactivation have been drawn based only on the protein sequence homology between (6–4) photolyase and CPD photolyase and therefore remain hypothetic [47].

Although the (6–4) photolyase enzyme binds to both DNA containing only (6–4)PP and DNA containing the Dewar isomer, its repair activity on the latter form is very low [99,107]. The enzyme's efficiency in repairing *cis–syn* CPDs is also negligible [17,107]. Even the overall quantum yield of repair of (6–4)PPs, $\Phi = 0.11$, is significantly lower than that of CPD repair by CPD photolyase under comparable experimental conditions ($\Phi = 0.42$ for *E. coli* CPD photolyase) [106]. Nevertheless, the enzyme faithfully restores various (6–4)PPs, namely T-64-T and T-64-C, to the original bases despite the difference in the functional group at the C(4) of the 3′-base [106,192]. These results strongly suggest that the transfer of the amino or hydroxyl group of the (6–4)PP is an intramolecular reaction within the substrate.

The absolute action spectrum of enzyme deficient of second chromophore and with the flavin cofactor in its fully reduced form closely matches the absorption spectrum of $FADH^{-}$ in the 350–600-nm region [106, 107]. Oxidation of $FADH^{-}$ cofactor to the neutral radical or fully oxidized form results in a significant reduction in repair efficiency. These results suggest that the enzyme with the fully reduced flavin is the catalytically active one. This similarity to CPD photolyase, together with the finding that the oxetane species (that is known to be intermediating the formation of a (6–4)PP) is unstable at temperatures above −80 °C, led Kim et al. [99] to propose that the equilibrium between the (6–4)PP and oxetane is shifted toward the latter upon enzyme binding. Subsequent electron transfer from $FADH^{-}$ to the oxetane could thus lead to oxetane splitting by an analogous mechanism to that proposed for CPD photorepair (see Fig. 4B) to give a neutral base and a base anion radical. The latter restores its electron to the $FADH^{\bullet}$, resulting in the fully repaired bases. On the basis of recent laser-flash photolysis, fluorescence quenching, and product analysis experiments, Joseph et al. [193] and Joseph and Falvey [194] and have demonstrated that various model compounds for the oxetane intermediate indeed undergo a cycloreversion reaction upon reductive electron transfer sensitized by strong electron donors such as *N*,*N*,*N*′,*N*′-tetramethylbenzidine.

An implicit assumption in the mechanism depicted in Fig. 4B is that the binding energy of the (6–4) photolyase enzyme to the (6–4)PP is sufficient to perturb the (6–4)PP $\rightleftarrows$ oxetane equilibrium in favor of the latter. Based on results from quantum-chemical computations, Heelis and Liu [195] questioned that the binding energy between the

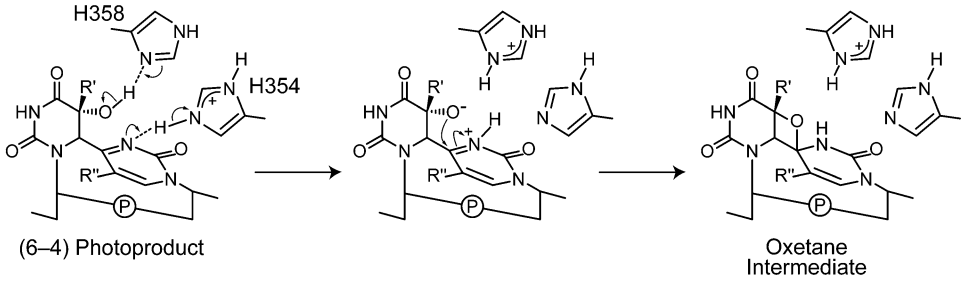

Fig. 7. The proposed mechanism for oxetane intermediate formation in (6–4) photolyase.

enzyme and substrate could compensate for the (positive) energy difference between the oxetane and the (6–4)PP (14.5–16 kcal/mol). Their calculations, however, were performed without taking into account the restraining effect of the sugar-phosphate backbone that could, in principle, strongly affect the predicted energy gap by straining either one or both structures. Interaction of critically placed amino acid side chains might further stabilize the oxetane intermediate relative to the (6–4)PP. Specifically, interactions between the highly conserved amino acid residues E304, D397, and D399 of the *D. melanogaster* (6–4) photolyase have been proposed by Zhao et al. [107]. The respective carboxylates (E279, D372, and D374) of *E. coli* CPD photolyase are found at the substrate-binding site, and hence would be in a position where they could act as general acid or base to facilitate the proposed oxetane intermediate provided, again in analogy to CPD photolyase, that the (6–4)PP lesion is extruded from the DNA duplex.

Hitomi et al. [196] might actually have been successful in finding the specific residues active in substrate binding to *X. laevis* (6–4) photolyase. They used a different approach by finding those amino acid residues within the regions comprising the proposed active site and the FAD-binding site of *X. laevis* (6–4) photolyase that are *not* found in CPD photolyases but are conserved among other (6–4) photolyases. Four amino acid residues that are

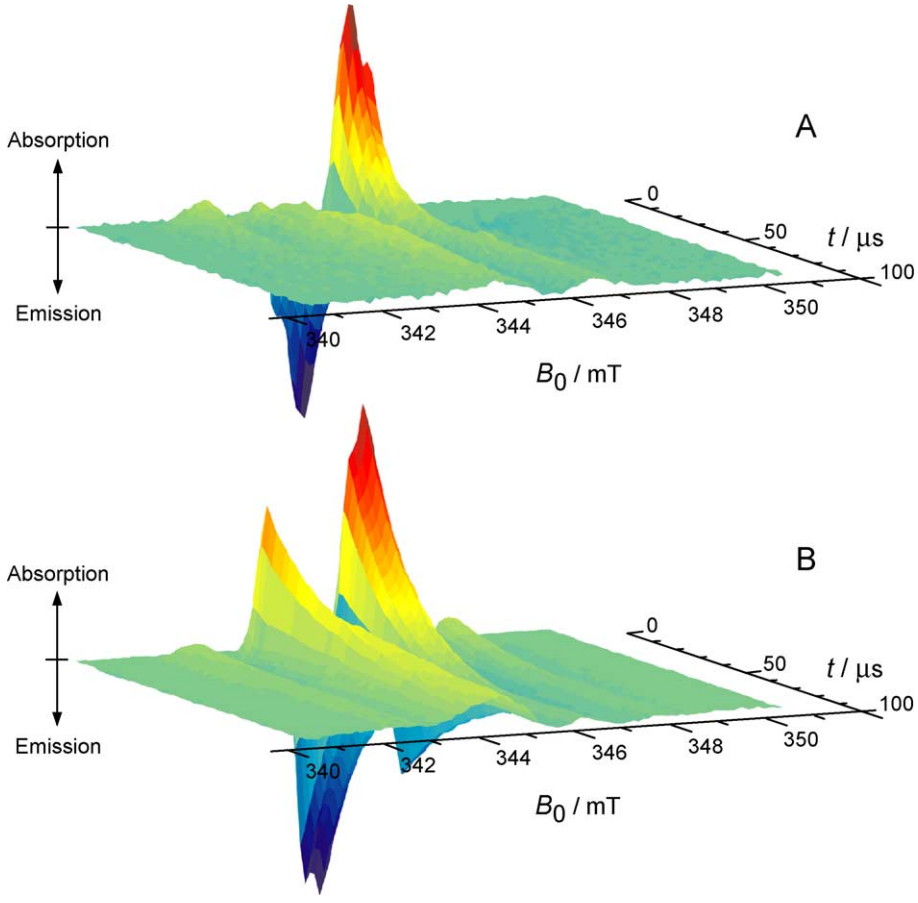

Fig. 8. Two-dimensional time-resolved EPR data sets of (A) *X. laevis* (6–4) photolyase, and (B) *E. coli* CPD photolyase, recorded at $T = 278$ K following pulsed laser excitation at 440 nm.

specific to (6–4) photolyases, Q288, H354, L355, and H358, and two conserved tryptophans, W291 and W398 (equivalent to W277 and W384 in *E. coli* CPD photolyase), were substituted with alanine. Only the L355A mutant had a lower affinity for the substrate, which suggested a hydrophobic interaction with the (6–4)PP. Both the H354A and H358A mutants resulted in an almost complete loss of repair activity, while W291A and W398A mutants retained some activity. In a structural model of the DNA-binding domain of *X. laevis* (6–4) photolyase that was constructed using the crystal structure of *E. coli* CPD photolyase as a starting point, H354, L355, and H358 are in close contact to the (6–4)PP. It was therefore proposed that the two histidines are crucial for the activity and catalyze the intermediate formation by a mechanism outlined in Fig. 7. In the docking model, the locations of H354 and H358 would allow hydrogen bonding to the N(3) of the 3′-pyrimidone and the hydroxyl group on the 5′-pyrimidine, respectively. Therefore, H358 could abstract a proton from the 5-OH group of the 5′-base, and at the same time, H354 could protonate the N(3) of the 3′-base to generate a highly electrophilic iminium ion. A nucleophilic attack to the cationic 3′-C(4) by the oxygen anion lone pair would result in the formation of the oxetane intermediate. The observation of a marked pH dependence of the (6–4)PP photorepair and an isotope effect upon H → D exchange are in accord with such a mechanism.

7.3. Photoactivation of the flavin cofactor

The photoactivation of the flavin cofactor has recently been studied in *X. laevis* (6–4) photolyase by time-resolved EPR spectroscopy with a high time resolution in the 50-ns range [197]. Isolation and purification typically renders the FAD cofactor in this enzyme fully oxidized. Upon photoexcitation with pulsed laser light of 440 nm, a radical-pair EPR spectrum with a characteristic spin-polarization pattern was observed (see Fig. 8). Comparison of this signal with the respective EPR signal arising from photoactivation of *E. coli* CPD photolyase revealed pronounced differences, mainly in the central regions of the spectra. Note that in these experiments, the electron-spin polarization pattern of the radical-pair signal reflects the spin state of the radical-pair precursor, which is a triplet state of FAD^{ox} generated by intersystem crossing from the excited singlet state, $*FAD^{ox}$.

The assignment of the signal contributions of the individual radical-pair halves has been accomplished from their characteristic resonance positions in the EPR spectrum, which is determined by their individual *g*-values. The **g**-matrix represents a global probe of the spatial and electronic structure of a paramagnetic species and allows for an unambiguous identification of a specific radical by EPR. Precise measurements of the principal values of the **g**-matrix of $FADH^{\bullet}$ in *E. coli* CPD photolyase were obtained from high-frequency/high-field EPR at 90 GHz/3.4 T [160] and 360 GHz/12.8 T (see Fig. 9) [198]. Only at 360 GHz the small anisotropy of the **g**-matrix of $FADH^{\bullet}$ could be resolved, yielding the principal values, $g_X = 2.00431(5)$, $g_Y = 2.00360(5)$, and $g_Z = 2.00217(7)$. The resulting average value, $g = 2.00336(5)$, confirms that obtained previously from 95-GHz EPR [160].

The broad spectral wings of the transient EPR spectrum of the radical-pair species in *X. laevis* (6–4) photolyase are centered at $g = 2.0034 \pm 0.0003$. This value is characteristic for the flavin-semiquinone cofactor in the neutral radical form, $FADH^{\bullet}$. The narrow emissive/absorptive polarized feature of the signal centered at $g = 2.0048 \pm 0.0003$ was assigned to a neutral (deprotonated) tyrosine radical, for which average *g*-values of $2.0045 \le g \le 2.0050$ are typically expected [199]. A tryptophan radical, by comparison, would show resonances centered at $g \approx 2.0025$ [200]. The tyrosine-radical signal was observed within 100 ns of pulsed laser excitation. Intermediate tryptophanyl radicals in (6–4) photolyase have not been detected. This indicates either $W^{\bullet}$ lifetimes of less than 100 ns or the presence of an electron-transfer pathway that is different from the one proposed for flavin photoactivation in CPD photolyases [109].

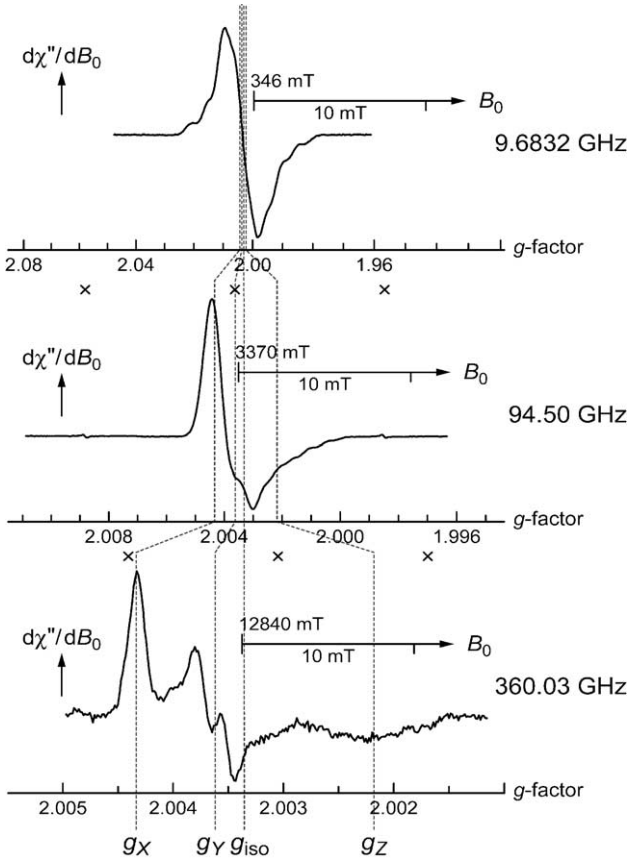

Fig. 9. Continuous-wave EPR spectra of the flavin cofactor of *E. coli* CPD photolyase in its neutral semiquinone form recorded at various combinations of the microwave frequency and the corresponding magnetic field. Spectra were recorded at 80 K (top curve, Ref. [160]), 150 K (middle curve, Ref. [160]) and 200 K (bottom curve, Ref. [198]).

8. Concluding remarks

To summarize, it is fair to state that a wealth of information on photolyase-mediated DNA repair has been obtained from the combined efforts of biologists, biochemists, molecular biologists and biophysicists, both in experiment and theory. Nevertheless, many key aspects of the repair reaction remain hypothetic. With regard to a thorough understanding of electron-transfer between the flavin cofactor and the DNA lesion, the three-dimensional structure of a complex comprising functionally competent enzyme bound to photodamaged DNA is urgently required, as is a structure of the (6–4) photolyase enzyme itself. Important questions that remain to be answered are: How does photolyase recognize CPDs and (6–4)PPs in DNA? What are the time constants and exact modes of splitting of CPDs and (6–4)PPs in the enzyme? What are the precise differences between CPD photolyase and (6–4) photolyase regarding substrate binding and DNA repair? Why are the cryptochromes, despite their high protein-sequence homology to (6–4) photolyase, incapable of repairing UV-induced DNA lesions? Could they, by highly specific protein manipulation, be induced to repair DNA? This could lead to novel therapeutic methods to repair DNA damages in humans, alternative to first successful approaches in which photolyase for prophylactic treatment of heavily sunlight-exposed human skin was utilized [201]. Modern biophysical characterization methods, if consequently applied to these issues, might substantially contribute to unraveling the remaining secrets of photoenzymatic DNA repair, now that well-defined protein samples are available that may be modified nearly at will.

Acknowledgements

Critical reading of this manuscript by Gerald Richter, Robert Bittl, Christopher W.M. Kay and Erik Schleicher is gratefully acknowledged. It is a pleasure to thank Professor Robert Bittl and Professor Klaus Möbius (Free University Berlin), and Dr. Gerald Richter and Professor Adelbert Bacher (Technical University Munich) for their support. Studies at the Free University Berlin were supported by the VolkswagenStiftung (grant I/77100) and the Deutsche Forschungsgemeinschaft (Sonderforschungsbereich 498 (TP A2) and Priority Program 1051 "High-Field EPR in Biology, Chemistry and Physics").

References

[1] E.C. Friedberg, G.C. Walker, W. Siede, DNA Repair and Mutagenesis, ASM Press, Washington, DC, 1995.
[2] H. Slaper, G.J.M. Velders, J.S. Daniel, F.R. de Gruijl, J.C. van der Leun, Estimates of ozone depletion and skin cancer incidence to examine the Vienna Convention achievements, Nature (Lond.) 384 (1996) 256–258.
[3] R.P. Kane, Ozone depletion, related UVB changes and increased skin cancer incidence, Int. J. Climatol. 18 (1998) 457–472.
[4] H. Slaper, G.J.M. Velders, J. Matthijsen, Ozone depletion and skin cancer incidence: a source risk approach, J. Hazard. Mater. 61 (1998) 77–84.
[5] A.A. Vink, L. Roza, Biological consequences of cyclobutane pyrimidine dimers, J. Photochem. Photobiol., B Biol. 65 (2001) 101–104.
[6] J.-S. Taylor, DNA, sunlight and skin cancer, Pure Appl. Chem. 67 (1995) 183–190.
[7] J.A. Lippke, L.K. Gordon, D.E. Brash, W.A. Haseltine, Distribution of UV light-induced damage in a defined sequence of human DNA: detection of alkaline-sensitive lesions at pyrimidine nucleoside-cytidine sequences, Proc. Natl. Acad. Sci. U. S. A. 78 (1981) 3388–3392.
[8] D.E. Brash, W.A. Haseltine, UV-induced mutation hotspots occur at DNA damage hotspots, Nature (Lond.) 298 (1982) 189–192.
[9] V.I. Lyamichev, M.D. Frank-Kamenetskii, V.N. Soyfer, Protection against UV-induced pyrimidine dimerization in DNA by triplex formation, Nature (Lond.) 344 (1990) 568–570.
[10] V.I. Lyamichev, Unusual conformation of $(dA)_n.(dT)_n$-tracts as revealed by cyclobutane thymine–thymine dimer formation, Nucleic Acids Res. 19 (1991) 4491–4496.
[11] J.R. Pehrson, L.H. Cohen, Effects of DNA looping on pyrimidine dimer formation, Nucleic Acids Res. 20 (1992) 1321–1324.
[12] E. Sage, Distribution and repair of photolesions in DNA: genetic consequences and the role of sequence context, Photochem. Photobiol. 57 (1993) 163–174.
[13] S. Tornaletti, G.P. Pfeifer, UV damage and repair mechanisms in mammalian cells, BioEssays 18 (1996) 221–228.
[14] M.M. Becker, Z. Wang, Origin of ultraviolet damage in DNA, J. Mol. Biol. 210 (1989) 429–438.
[15] P.C. Hanawalt, Transcription-coupled repair and human disease, Science 266 (1994) 1957–1958.
[16] B.A. Donahue, S. Yin, J.-S. Taylor, D. Reines, P.C. Hanawalt, Transcript cleavage by RNA polymerase II arrested by a cyclobutane pyrimidine dimer in the DNA template, Proc. Natl. Acad. Sci. U. S. A. 91 (1994) 8502–8506.
[17] E. Otoshi, T. Yagi, T. Mori, T. Matsunaga, O. Nikaido, S.-T. Kim, K. Hitomi, M. Ikenaga, T. Todo, Respective roles of cyclobutane pyrimidine dimers, (6–4) photoproducts, and minor photoproducts in ultraviolet mutagenesis of repair-deficient xeroderma pigmentosum A cells, Cancer Res. 60 (2000) 1729–1735.
[18] Y.-H. You, D.-H. Lee, J.-H. Yoon, S. Nakajima, A. Yasui, G.P. Pfeifer, Cyclobutane pyrimidine dimers are responsible for the vast majority of mutations induced by UVB irradiation in mammalian cells, J. Biol. Chem. 276 (2001) 44688–44694.
[19] B.A. Gilchrest, M.S. Eller, A.C. Geller, M. Yaar, The pathogenesis of melanoma induced by ultraviolet radiation, N. Engl. J. Med. 340 (1999) 1341–1348.
[20] J.E. Cleaver, E. Crowley, UV damage, DNA repair and skin carcinogenesis, Front. Biosci. 7 (2002) 1024–1043.
[21] E. Guzman, J.L. Langowski, L. Owen-Schaub, Mad dogs, Englishmen and apoptosis: the role of cell death in UV-induced skin cancer, Apoptosis 8 (2003) 315–325.
[22] C. Jhappan, F.P. Noonan, G. Merlino, Ultraviolet radiation and cutaneous malignant melanoma, Oncogene 22 (2003) 3099–3112.
[23] Y.-H. You, P.E. Szabó, G.P. Pfeifer, Cyclobutane pyrimidine dimers form preferentially at the major p53 mutational hotspot in UVB-induced mouse skin tumors, Carcinogenesis (Lond.) 21 (2000) 2113–2117.
[24] S. Adimoolam, J.M. Ford, p53 and regulation of DNA damage recognition during nucleotide excision repair, DNA Repair 2 (2003) 947–954.
[25] A. Yasui, S.J. McCready, Alternative repair pathways for UV-induced DNA damage, BioEssays 20 (1998) 291–297.
[26] C.S. Rupert, Photoreactivation of transforming DNA by an enzyme from baker's yeast, J. Gen. Physiol. 43 (1960) 573–595.

[27] C.S. Rupert, Photoenzymatic repair of ultraviolet damage in DNA: I. Kinetics of the reaction, J. Gen. Physiol. 45 (1962) 703–724.
[28] S. Minato, H. Werbin, Excitation and fluorescence spectra of the chromophore associated with the DNA-photoreactivating enzyme from the blue-green alga *Anacystis nidulans*, Photochem. Photobiol. 15 (1972) 97–100.
[29] G.B. Sancar, DNA photolyases: physical properties, action mechanism, and roles in dark repair, Mutat. Res. 236 (1990) 147–160.
[30] A. Sancar, Photolyase: DNA repair by photoinduced electron transfer, in: P.E. Mariano (Ed.), Advances in Electron Transfer Chemistry, JAI Press, London, 1992, pp. 215–272.
[31] P.F. Heelis, S.-T. Kim, T. Okamura, A. Sancar, The photo repair of pyrimidine dimers by DNA photolyase and model systems, J. Photochem. Photobiol., B Biol. 17 (1993) 219–228.
[32] S.-T. Kim, A. Sancar, Photochemistry, photophysics, and mechanism of pyrimidine dimer repair by DNA photolyase, Photochem. Photobiol. 57 (1993) 895–904.
[33] A. Sancar, Structure and function of DNA photolyase, Biochemistry 33 (1994) 2–9.
[34] P.F. Heelis, R.F. Hartman, S.D. Rose, Photoenzymic repair of UV-damaged DNA: a chemist's perspective, Chem. Soc. Rev. 24 (1995) 289–297.
[35] T. Carell, Sunlight-damaged DNA repaired with sunlight, Angew. Chem., Int. Ed. Engl. 34 (1995) 2491–2494.
[36] P.F. Heelis, R.F. Hartman, S.D. Rose, Energy and electron transfer processes in flavoprotein-mediated DNA repair, J. Photochem. Photobiol., A Chem. 95 (1996) 89–98.
[37] A. Sancar, No "end of history" for photolyases, Science 272 (1996) 48–49.
[38] X. Zhao, D. Mu, (6–4) Photolyase: light-dependent repair of DNA damage, Histol. Histopathol. 13 (1998) 1179–1182.
[39] F. Thoma, Light and dark in chromatin repair: repair of UV-induced DNA lesions by photolyase and nucleotide excision repair, EMBO J. 18 (1999) 6585–6598.
[40] T. Todo, Functional diversity of the DNA photolyase/blue light receptor family, Mutat. Res. 434 (1999) 89–97.
[41] G.B. Sancar, Enzymatic photoreactivation: 50 years and counting, Mutat. Res. 451 (2000) 25–37.
[42] J. Deisenhofer, DNA photolyases and cryptochromes, Mutat. Res. 460 (2000) 143–149.
[43] T. Carell, L.T. Burgdorf, L.M. Kundu, M. Cichon, The mechanism of action of DNA photolyases, Curr. Opin. Chem. Biol. 5 (2001) 491–498.
[44] R.P. Sinha, D.-P. Häder, UV-induced DNA damage and repair: a review, Photochem. Photobiol. Sci. 1 (2002) 225–236.
[45] C.L. Thompson, A. Sancar, Photolyase/cryptochrome blue-light photoreceptors use photon energy to repair DNA and reset the circadian clock, Oncogene 21 (2002) 9043–9056.
[46] A. Sancar, Structure and function of DNA photolyase and cryptochrome blue-light photoreceptors, Chem. Rev. 103 (2003) 2203–2237.
[47] T. Todo, H. Ryo, K. Yamamoto, H. Toh, T. Inui, H. Ayaki, T. Nomura, M. Ikenaga, Similarity among the *Drosophila* (6–4) photolyase, a human photolyase homolog, and the DNA photolyase-blue-light photoreceptor family, Science 272 (1996) 109–112.
[48] D.S. Hsu, X. Zhao, S. Zhao, A. Kazantsev, R.-P. Wang, T. Todo, Y.-F. Wei, A. Sancar, Putative human blue-light photoreceptors hCRY1 and hCRY2 are flavoproteins, Biochemistry 35 (1996) 13871–13877.
[49] P.J. van der Spek, K. Kobayashi, D. Bootsma, M. Takao, A.P.M. Eker, A. Yasui, Cloning, tissue expression, and mapping of a human photolyase homolog with similarity to plant blue-light receptors, Genomics 37 (1996) 177–182.
[50] T. Todo, H. Tsuji, E. Otoshi, K. Hitomi, S.-T. Kim, M. Ikenaga, Characterization of a human homolog of (6–4) photolyase, Mutat. Res. 384 (1997) 195–204.
[51] P. Emery, W.V. So, M. Kaneko, J.C. Hall, M. Rosbash, CRY, a *Drosophila* clock and light-regulated cryptochrome, is a major contributor to circadian rhythm resetting and photosensitivity, Cell (Cambridge, MA) 95 (1998) 669–679.
[52] Y. Miyamoto, A. Sancar, Vitamin B_2-based blue-light photoreceptors in the retinohypothalamic tract as the photoactive pigments for setting the circadian clock in mammals, Proc. Natl. Acad. Sci. U. S. A. 95 (1998) 6097–6102.
[53] P.F. Devlin, S.A. Kay, Cryptochromes—bringing the blues to circadian rhythms, Trends Cell Biol. 9 (1999) 295–298.
[54] A. Sancar, Cryptochrome: the second photoactive pigment in the eye and its role in circadian photoreception, Annu. Rev. Biochem. 69 (2000) 31–67.
[55] P.F. Devlin, S.A. Kay, Circadian photoperception, Annu. Rev. Physiol. 63 (2001) 677–694.
[56] A.R. Cashmore, Cryptochromes: enabling plants and animals to determine circadian time, Cell (Cambridge, MA) 114 (2003) 537–543.
[57] R.D. Wood, M. Mitchell, J. Sgouros, T. Lindahl, Human DNA repair genes, Science 291 (2001) 1284–1289.
[58] W. Schul, J. Jans, Y.M.A. Rijksen, K.H.M. Klemann, A.P.M. Eker, J. de Wit, O. Nikaido, S. Nakajima, A. Yasui, J.H.J. Hoeijmakers, G.T.J. van der Horst, Enhanced repair of cyclobutane pyrimidine dimers and improved UV resistance in photolyase transgenic mice, EMBO J. 21 (2002) 4719–4729.
[59] C.C.-K. Chao, Lack of DNA enzymatic photoreactivation in HeLa cell-free extracts, FEBS Lett. 336 (1993) 411–416.
[60] Y.F. Li, S.-T. Kim, A. Sancar, Evidence for lack of DNA photoreactivating enzyme in humans, Proc. Natl. Acad. Sci. U. S. A. 90 (1993) 4389–4393.
[61] R.D. Ley, Photoreactivation in humans, Proc. Natl. Acad. Sci. U. S. A. 90 (1993) 4337.
[62] A. Yasui, A.P.M. Eker, S. Yasuhira, H. Yajima, T. Kobayashi, M. Oikawa, A. Oikawa, A new class of DNA photolyases present in various organisms including aplacental mammals, EMBO J. 13 (1994) 6143–6151.
[63] S. Kanai, R. Kikuno, H. Toh, H. Ryo, T. Todo, Molecular evolution of the photolyase-blue-light photoreceptor family, J. Mol. Evol. 45 (1997) 535–548.
[64] K. Hitomi, K. Okamoto, H. Daiyasu, H. Miyashita, S. Iwai, H. Toh, M. Ishiura, T. Todo, Bacterial cryptochrome and photolyase: characterization of two photolyase-like genes of *Synechocystis* sp. PCC6803, Nucleic Acids Res. 28 (2000) 2353–2362.
[65] S. Yasuhira, A. Yasui, Visible light-inducible photolyase gene from the goldfish *Carassius auratus*, J. Biol. Chem. 267 (1992) 25644–25647.
[66] T. Todo, H. Ryo, H. Takemori, H. Toh, T. Nomura, S. Kondo, High-level expression of the photorepair gene in *Drosophila* ovary and its evolutionary implications, Mutat. Res. 315 (1994) 213–228.
[67] M. Ahmad, J.A. Jarillo, L.J. Klimczak, L.G. Landry, T. Peng, R.L. Last, A.R. Cashmore, An enzyme similar to animal type II photolyases mediates photoreactivation in *Arabidopsis*, Plant Cell 9 (1997) 199–207.
[68] O. Kleiner, J. Butenandt, T. Carell, A. Batschauer, Class II DNA photolyase from *Arabidopsis thaliana* contains FAD as a cofactor, Eur. J. Biochem. 264 (1999) 161–167.
[69] C.-Z. Jiang, J. Yee, D.L. Mitchell, A.B. Britt, Photorepair mutants of *Arabidopsis*, Proc. Natl. Acad. Sci. U. S. A. 94 (1997) 7441–7445.
[70] S. Takahashi, N. Nakajima, H. Saji, N. Kondo, Diurnal change of cucumber CPD photolyase gene (*CsPHR*) expression and its physiological role in growth under UV-B irradiation, Plant Cell Physiol. 43 (2002) 342–349.
[71] T. Hirouchi, S. Nakajima, T. Najrana, M. Tanaka, T. Matsunaga, J. Hidema, M. Teranishi, T. Fujino, T. Kumagai, K. Yamamoto, A gene for a class II DNA photolyase from *Oryza sativa*: cloning of the cDNA by dilution-amplification, Mol. Gen. Genomics 269 (2003) 508–516.

[72] K.A. O'Connor, M.J. McBride, M. West, H. Yu, L. Trinh, K. Yuan, T. Lee, D.R. Zusman, Photolyase of *Myxococcus xanthus*, a gram-negative eubacterium, is more similar to photolyases found in archaea and "higher" eukaryotes than to photolyases of other eubacteria, J. Biol. Chem. 271 (1996) 6252–6259.
[73] J.L. Petersen, D.W. Lang, G.D. Small, Cloning and characterization of a class II DNA photolyase from *Chlamydomonas*, Plant Mol. Biol. 40 (1999) 1063–1071.
[74] V. Srinivasan, W.M. Schnitzlein, D.N. Tripathy, Fowlpox virus encodes a novel DNA repair enzyme, CPD-photolyase, that restores infectivity of UV light-damaged virus, J. Virol. 75 (2001) 1681–1688.
[75] C.J. Bennett, M. Webb, D.O. Willer, D.H. Evans, Genetic and phylogenetic characterization of the type II cyclobutane pyrimidine dimer photolyases encoded by Leporipoxviruses, Virology 315 (2003) 10–19.
[76] A. Batschauer, A plant gene for photolyase: an enzyme catalyzing the repair of UV-light-induced DNA damage, Plant J. 4 (1993) 705–709.
[77] N. Iwatsuki, C.O. Joe, H. Werbin, Evidence that deoxyribonucleic acid photolyase from baker's yeast is a flavoprotein, Biochemistry 19 (1980) 1172–1176.
[78] A. Sancar, G.B. Sancar, *Escherichia coli* DNA photolyase is a flavoprotein, J. Mol. Biol. 172 (1984) 223–227.
[79] M.S. Jorns, G.B. Sancar, A. Sancar, Identification of a neutral flavin radical and characterization of a second chromophore in *Escherichia coli* DNA photolyase, Biochemistry 23 (1984) 2673–2679.
[80] A.P.M. Eker, P. Kooiman, J.K.C. Hessels, A. Yasui, DNA photoreactivating enzyme from the cyanobacterium *Anacystis nidulans*, J. Biol. Chem. 265 (1990) 8009–8015.
[81] A.P.M. Eker, H. Yajima, A. Yasui, DNA photolyase from the fungus *Neurospora crassa*. Purification, characterization and comparison with other photolyases, Photochem. Photobiol. 60 (1994) 125–133.
[82] S.-T. Kim, K. Malhotra, H. Ryo, A. Sancar, T. Todo, Purification and characterization of *Drosophila melanogaster* photolyase, Mutat. Res. 363 (1996) 97–104.
[83] T. Todo, S.-T. Kim, K. Hitomi, E. Otoshi, T. Inui, H. Morioka, H. Kobayashi, E. Ohtsuka, H. Toh, M. Ikenaga, Flavin adenine dinucleotide as a chromophore of the *Xenopus* (6–4) photolyase, Nucleic Acids Res. 25 (1997) 764–768.
[84] R. Kato, K. Hasegawa, Y. Hidaka, S. Kuramitsu, T. Hoshino, Characterization of a thermostable DNA photolyase from an extremely thermophilic bacterium, *Thermus thermophilus* HB27, J. Bacteriol. 179 (1997) 6499–6503.
[85] V. Massey, Introduction: flavoprotein structure and mechanism, FASEB J. 9 (1995) 473–475.
[86] M.W. Fraaije, A. Mattevi, Flavoenzymes: diverse catalysts with recurrent features, Trends Biochem. Sci. 25 (2000) 126–132.
[87] C.W.M. Kay, S. Weber, EPR of radical intermediates in flavoenzymes, in: B.C. Gilbert, M.J. Davies, D.M. Murphy (Eds.), Electron Paramagnetic Resonance, Royal Society of Chemistry, Cambridge, UK, 2002, pp. 222–253.
[88] J.L. Johnson, S. Hamm-Alvarez, G. Payne, G.B. Sancar, K.V. Rajagopalan, A. Sancar, Identification of the second chromophore of *Escherichia coli* and yeast DNA photolyases as 5,10-methenyltetrahydrofolate, Proc. Natl. Acad. Sci. U. S. A. 85 (1988) 2046–2050.
[89] Y.F. Li, A. Sancar, Cloning, sequencing, expression and characterization of DNA photolyase from *Salmonella typhimurium*, Nucleic Acids Res. 19 (1991) 4885–4890.
[90] E.N. Worthington, I.H. Kavaklý, G. Berrocal-Tito, B.E. Bondo, A. Sancar, Purification and characterization of three members of the photolyase/cryptochrome family blue-light photoreceptors from *Vibrio cholerae*, J. Biol. Chem. 278 (2003) 39143–39154.
[91] G.B. Sancar, F.W. Smith, P.F. Heelis, Purification of the yeast *PHR1* photolyase from an *Escherichia coli* overproducing strain and characterization of the intrinsic chromophores of the enzyme, J. Biol. Chem. 262 (1987) 15457–15465.
[92] H. Yajima, H. Inoue, A. Oikawa, A. Yasui, Cloning and functional characterization of a eucaryotic DNA photolyase gene from *Neurospora crassa*, Nucleic Acids Res. 19 (1991) 5359–5362.
[93] A. Yasui, M. Takao, A. Oikawa, A. Kiener, C.T. Walsh, A.P.M. Eker, Cloning and characterization of a photolyase gene from the cyanobacterium *Anacystis nidulans*, Nucleic Acids Res. 16 (1988) 4447–4463.
[94] A.P.M. Eker, R.H. Dekker, W. Berends, Photoreactivating enzyme from *Streptomyces griseus*: IV. On the nature of the chromophoric cofactor in *Streptomyces griseus* photoreactivating enzyme, Photochem. Photobiol. 33 (1981) 65–72.
[95] A.P.M. Eker, J.K.C. Hessels, J. van de Velde, Photoreactivating enzyme from the green alga *Scenedesmus acutus*. Evidence for the presence of two different flavin chromophores, Biochemistry 27 (1988) 1758–1765.
[96] T. Iwasa, S. Tokutomi, F. Tokunaga, Photoreactivation of *Halobacterium halobium*: action spectrum and role of pigmentation, Photochem. Photobiol. 47 (1988) 267–270.
[97] A. Kiener, I. Husain, A. Sancar, C. Walsh, Purification and properties of *Methanobacterium thermoautotrophicum* DNA photolyase, J. Biol. Chem. 264 (1989) 13880–13887.
[98] T. Todo, H. Takemori, H. Ryo, M. Ihara, T. Matsunaga, O. Nikaido, K. Sato, T. Nomura, A new photoreactivating enzyme that specifically repairs ultraviolet light-induced (6–4) photoproducts, Nature (Lond.) 361 (1993) 371–374.
[99] S.-T. Kim, K. Malhotra, C.A. Smith, J.-S. Taylor, A. Sancar, Characterization of (6–4) photoproduct DNA photolyase, J. Biol. Chem. 269 (1994) 8535–8540.
[100] S.-T. Kim, K. Malhotra, J.-S. Taylor, A. Sancar, Purification and partial characterization of (6–4) photoproduct DNA photolyase from *Xenopus laevis*, Photochem. Photobiol. 63 (1996) 292–295.
[101] Y. Kobayashi, T. Ishikawa, J. Hirayama, H. Daiyasu, S. Kanai, H. Toh, I. Fukuda, T. Tsujimura, N. Terada, Y. Kamei, S. Yuba, S. Iwai, T. Todo, Molecular analysis of zebrafish photolyase/cryptochrome family: two types of cryptochromes present in zebrafish, Genes Cells 5 (2000) 725–738.
[102] J.-J. Chen, D.L. Mitchell, A.B. Britt, A light-dependent pathway for the elimination of UV-induced pyrimidine (6–4) pyrimidinone photoproducts in *Arabidopsis*, Plant Cell 6 (1994) 1311–1317.
[103] S. Nakajima, M. Sugiyama, S. Iwai, K. Hitomi, E. Otoshi, S.-T. Kim, C.-Z. Jiang, T. Todo, A.B. Britt, K. Yamamoto, Cloning and characterization of a gene (UVR3) required for photorepair of 6–4 photoproducts in *Arabidopsis thaliana*, Nucleic Acids Res. 26 (1998) 638–644.
[104] S. McCready, L. Marcello, Repair of UV damage in *Halobacterium salinarum*, Biochem. Soc. Trans. 31 (2003) 694–698.
[105] H.C. Schröder, A. Krasko, D. Gundacker, S.P. Leys, I.M. Müller, W.E.G. Müller, Molecular and functional analysis of the (6–4) photolyase from the hexactinellid *Aphrocallistes vastus*, Biochim. Biophys. Acta 1651 (2003) 41–49.
[106] K. Hitomi, S.-T. Kim, S. Iwai, N. Harima, E. Otoshi, M. Ikenaga, T. Todo, Binding and catalytic properties of *Xenopus* (6–4) photolyase, J. Biol. Chem. 272 (1997) 32591–32598.
[107] X. Zhao, J. Liu, D.S. Hsu, S. Zhao, J.-S. Taylor, A. Sancar, Reaction mechanism of (6–4) photolyase, J. Biol. Chem. 272 (1997) 32580–32590.
[108] C. Walsh, Naturally occurring 5-deazaflavin coenzymes: biological redox roles, Acc. Chem. Res. 19 (1986) 216–221.
[109] H.-W. Park, S.-T. Kim, A. Sancar, J. Deisenhofer, Crystal structure of DNA photolyase from *Escherichia coli*, Science 268 (1995) 1866–1872.
[110] T. Tamada, K. Kitadokoro, Y. Higuchi, K. Inaka, A. Yasui, P.E. de Ruiter, A.P.M. Eker, K. Miki, Crystal structure of DNA photolyase from *Anacystis nidulans*, Nat. Struct. Biol. 4 (1997) 887–891.
[111] H. Komori, R. Masui, S. Kuramitsu, S. Yokoyama, T. Shibata, Y.

Inoue, K. Miki, Crystal structure of thermostable DNA photolyase: pyrimidine-dimer recognition mechanism, Proc. Natl. Acad. Sci. U. S. A. 98 (2001) 13560–13565.
[112] R.J. Roberts, X. Cheng, Base flipping, Annu. Rev. Biochem. 67 (1998) 181–198.
[113] W. Harm, H. Harm, C.S. Rupert, Analysis of photoenzymatic repair of UV lesions in DNA by single light flashes: II. In vivo studies with *Escherichia coli* cells and bacteriophage, Mutat. Res. 6 (1968) 371–385.
[114] A. Yasui, W. Laskowski, Determination of the number of photoreactivating enzyme molecules per haploid *Saccharomyces* cell, Int. J. Radiat. Biol. 28 (1975) 511–518.
[115] A. Fukui, K. Hieda, Y. Matsudaira, Light-flash analysis of the photoenzymic repair process in yeast cells: I. Determination of the number of photoreactivating enzyme molecules, Mutat. Res. 51 1978, pp. 435–439.
[116] G. Payne, M. Wills, C. Walsh, A. Sancar, Reconstitution of *Escherichia coli* photolyase with flavins and flavin analogues, Biochemistry 29 (1990) 5706–5711.
[117] G.B. Sancar, M.S. Jorns, G. Payne, D.J. Fluke, C.S. Rupert, A. Sancar, Action mechanism of *Escherichia coli* DNA photolyase: III. Photolysis of the enzyme–substrate complex and the absolute action spectrum, J. Biol. Chem. 262 (1987) 492–498.
[118] I. Husain, G.B. Sancar, S.R. Holbrook, A. Sancar, Mechanism of damage recognition by *Escherichia coli* DNA photolyase, J. Biol. Chem. 262 (1987) 13188–13197.
[119] I. Husain, A. Sancar, Binding of E. coli DNA photolyase to a defined substrate containing a single T◇T dimer, Nucleic Acids Res. 15 (1987) 1109–1120.
[120] G. Payne, A. Sancar, Absolute action spectrum of E-$FADH_2$ and E-$FADH_2$-MTHF forms of *Escherichia coli* DNA photolyase, Biochemistry 29 (1990) 7715–7727.
[121] G.B. Sancar, F.W. Smith, A. Sancar, Binding of *Escherichia coli* DNA photolyase to UV-irradiated DNA, Biochemistry 24 (1985) 1849–1855.
[122] G.B. Sancar, F.W. Smith, R. Reid, G. Payne, M. Levy, A. Sancar, Action mechanism of *Escherichia coli* DNA photolyase: I. Formation of the enzyme–substrate complex, J. Biol. Chem. 262 (1987) 478–485.
[123] Y.F. Li, A. Sancar, Active site of *Escherichia coli* DNA photolyase: mutations at Trp277 alter the selectivity of the enzyme without affecting the quantum yield of photorepair, Biochemistry 29 (1990) 5698–5706.
[124] M.E. Baer, G.B. Sancar, The role of conserved amino acids in substrate binding and discrimination by photolyase, J. Biol. Chem. 268 (1993) 16717–16724.
[125] S.-T. Kim, K. Malhotra, C.A. Smith, J.-S. Taylor, A. Sancar, DNA photolyase repairs the *trans–syn* cyclobutane thymine dimer, Biochemistry 32 (1993) 7065–7068.
[126] S.-T. Kim, A. Sancar, Effect of base, pentose, and phosphodiester backbone structures on binding and repair of pyrimidine dimers by *Escherichia coli* DNA photolyase, Biochemistry 30 (1991) 8623–8630.
[127] J. van Noort, F. Orsini, A.P.M. Eker, C. Wyman, B. de Grooth, J. Greve, DNA bending by photolyase in specific and non-specific complexes studied by atomic force microscopy, Nucleic Acids Res. 27 (1999) 3875–3880.
[128] M. Baer, G.B. Sancar, Photolyases from *Saccharomyces cerevisiae* and *Escherichia coli* recognize common binding determinants in DNA containing pyrimidine dimers, Mol. Cell. Biol. 9 (1989) 4777–4788.
[129] B.J. Vande Berg, G.B. Sancar, Evidence for dinucleotide flipping by DNA photolyase, J. Biol. Chem. 273 (1998) 20276–20284.
[130] K.S. Christine, A.W. MacFarlane IV, K. Yang, R.J. Stanley, Cyclobutylpyrimidine dimer base flipping by DNA photolyase, J. Biol. Chem. 277 (2002) 38339–38344.
[131] D.B. Sanders, O. Wiest, A model for the enzyme–substrate complex of DNA photolyase and photodamaged DNA, J. Am. Chem. Soc. 121 (1999) 5127–5134.
[132] J. Hahn, M.-E. Michel-Beyerle, N. Rösch, Binding of pyrimidine model dimers to the photolyase enzyme: a molecular dynamics study, J. Phys. Chem., B 103 (1999) 2001–2007.
[133] J. Antony, D.M. Medvedev, A.A. Stuchebrukhov, Theoretical study of electron transfer between the photolyase catalytic cofactor $FADH^-$ and DNA thymine dimer, J. Am. Chem. Soc. 122 (2000) 1057–1065.
[134] S. Weber, G. Richter, E. Schleicher, A. Bacher, K. Möbius, C.W.M. Kay, Substrate binding to DNA photolyase studied by electron paramagnetic resonance spectroscopy, Biophys. J. 81 (2001) 1195–1204.
[135] A.W. MacFarlane IV, R.J. Stanley, Evidence of powerful substrate electric fields in DNA photolyase: implications for thymidine dimer repair, Biochemistry 40 (2001) 15203–15214.
[136] M.S. Jorns, B. Wang, S.P. Jordan, L.P. Chanderkar, Chromophore function and interaction in *Escherichia coli* DNA photolyase: reconstitution of the apoenzyme with pterin and/or flavin derivatives, Biochemistry 29 (1990) 552–561.
[137] S.P. Jordan, J.L. Alderfer, L.P. Chanderkar, M.S. Jorns, Reaction of *Escherichia coli* and yeast photolyases with homogeneous short-chain oligonucleotide substrates, Biochemistry 28 (1989) 8149–8153.
[138] J.P.M. Schelvis, M. Ramsey, O. Sokolova, C. Tavares, C. Cecala, K. Connell, S. Wagner, Y.M. Gindt, Resonance Raman and UV–vis spectroscopic characterization of $FADH^{\cdot}$ in the complex of photolyase with UV-damaged DNA, J. Phys. Chem., B 107 (2003) 12352–12362.
[139] D.H. Murgida, E. Schleicher, A. Bacher, G. Richter, P. Hildebrandt, Resonance Raman spectroscopic study of the neutral flavin radical complex of DNA photolyase from *Escherichia coli*, J. Raman Spectrosc. 32 (2001) 551–556.
[140] P.F. Heelis, A. Sancar, Photochemical properties of *Escherichia coli* DNA photolyase: a flash photolysis study, Biochemistry 25 (1986) 8163–8166.
[141] M.S. Jorns, E.T. Baldwin, G.B. Sancar, A. Sancar, Action mechanism of *Escherichia coli* DNA photolyase: II. Role of the chromophores in catalysis, J. Biol. Chem. 262 (1987) 486–491.
[142] G. Payne, P.F. Heelis, B.R. Rohrs, A. Sancar, The active form of *Escherichia coli* DNA photolyase contains a fully reduced flavin and not a flavin radical, both in vivo and in vitro, Biochemistry 26 (1987) 7121–7127.
[143] P.F. Heelis, G. Payne, A. Sancar, Photochemical properties of *Escherichia coli* DNA photolyase: selective photodecomposition of the second chromophore, Biochemistry 26 (1987) 4634–4640.
[144] M.S. Jorns, B. Wang, S.P. Jordan, DNA repair catalyzed by *Escherichia coli* DNA photolyase containing only reduced flavin: elimination of the enzyme's second chromophore by reduction with sodium borohydride, Biochemistry 26 (1987) 6810–6816.
[145] R.S.A. Lipman, M.S. Jorns, Direct evidence for singlet–singlet energy transfer in *Escherichia coli* DNA photolyase, Biochemistry 31 (1992) 786–791.
[146] T. Okamura, A. Sancar, P.F. Heelis, T.P. Begley, Y. Hirata, N. Mataga, Picosecond laser photolysis studies on the photorepair of pyrimidine dimers by DNA photolyase: 1. Laser photolysis of photolyase-2-deoxyuridine dinucleotide photodimer complex, J. Am. Chem. Soc. 113 (1991) 3143–3145.
[147] S.-T. Kim, P.F. Heelis, T. Okamura, Y. Hirata, N. Mataga, A. Sancar, Determination of rates and yields of interchromophore (folate → flaflavin) energy transfer and intermolecular (flavin → DNA) electron transfer in *Escherichia coli* photolyase by time-resolved fluorescence and absorption spectroscopy, Biochemistry 30 (1991) 11262–11270.
[148] S.-T. Kim, P.F. Heelis, A. Sancar, Energy transfer (deazaflavin → $FADH_2$) and electron transfer ($FADH_2$ → T◇T) kinetics in *Anacystis nidulans* photolyase, Biochemistry 31 (1992) 11244–11248.

[149] S. Hamm-Alvarez, A. Sancar, K.V. Rajagopalan, Role of enzyme-bound 5,10-methenyltetrahydropteroylpolyglutamate in catalysis by *Escherichia coli* DNA photolyase, J. Biol. Chem. 264 (1989) 9649–9656.
[150] S. Hamm-Alvarez, A. Sancar, K.V. Rajagopalan, The folate cofactor of *Escherichia coli* DNA photolyase acts catalytically, J. Biol. Chem. 265 (1990) 18656–18662.
[151] S.P. Jordan, M.S. Jorns, Evidence for a singlet intermediate in catalysis by *Escherichia coli* DNA photolyase and evaluation of substrate binding determinants, Biochemistry 27 (1988) 8915–8923.
[152] A.W. MacFarlane IV, R.J. Stanley, *Cis–syn* thymidine dimer repair by DNA photolyase in real time, Biochemistry 42 (2003) 8558–8568.
[153] S.-T. Kim, M. Volk, G. Rousseau, P.F. Heelis, A. Sancar, M.E. Michel-Beyerle, Laser flash photolysis on an intermediate in the repair of pyrimidine dimers by DNA photolyase, J. Am. Chem. Soc. 116 (1994) 3115–3116.
[154] T. Langenbacher, X. Zhao, G. Bieser, P.F. Heelis, A. Sancar, M.E. Michel-Beyerle, Substrate and temperature dependence of DNA photolyase repair activity examined with ultrafast spectroscopy, J. Am. Chem. Soc. 119 (1997) 10532–10536.
[155] S.T. Kim, A. Sancar, C. Essenmacher, G.T. Babcock, Evidence from photoinduced EPR for a radical intermediate during photolysis of cyclobutane thymine dimer by DNA photolyase, J. Am. Chem. Soc. 114 (1992) 4442–4443.
[156] Y.M. Gindt, E. Vollenbroek, K. Westphal, H. Sackett, A. Sancar, G.T. Babcock, Origin of the transient electron paramagnetic resonance signals in DNA photolyase, Biochemistry 38 (1999) 3857–3866.
[157] R.R. Rustandi, M.S. Jorns, Photoinduced spin-polarized radical pair formation in a DNA photolyase substrate complex at low temperature, Biochemistry 34 (1995) 2284–2288.
[158] J. Hahn, M.-E. Michel-Beyerle, N. Rösch, Conformation of the flavin adenine dinucleotide cofactor FAD in DNA-photolyase: a molecular dynamics study, J. Mol. Model. 4 (1998) 73–82.
[159] D. Medvedev, A.A. Stuchebrukhov, DNA repair mechanism by photolyase: electron transfer path from the photolyase catalytic cofactor $FADH^-$ to DNA thymine dimer, J. Theor. Biol. 210 (2001) 237–248.
[160] C.W.M. Kay, R. Feicht, K. Schulz, P. Sadewater, A. Sancar, A. Bacher, K. Möbius, G. Richter, S. Weber, EPR, ENDOR and TRIPLE resonance spectroscopy on the neutral flavin radical in *Escherichia coli* DNA Photolyase, Biochemistry 38 (1999) 16740–16748.
[161] S. Weber, K. Möbius, G. Richter, C.W.M. Kay, The electronic structure of the flavin cofactor in DNA photolyase, J. Am. Chem. Soc. 123 (2001) 3790–3798.
[162] S.-T. Kim, Y.F. Li, A. Sancar, The third chromophore of DNA photolyase: Trp-277 of *Escherichia coli* DNA photolyase repairs thymine dimers by direct electron transfer, Proc. Natl. Acad. Sci. U. S. A. 89 (1992) 900–904.
[163] M.P. Scannell, D.J. Fenick, S.-R. Yeh, D.E. Falvey, Model studies of DNA photorepair: reduction potentials of thymine and cytosine cyclobutane dimers measured by fluorescence quenching, J. Am. Chem. Soc. 119 (1997) 1971–1977.
[164] A.A. Voityuk, M.-E. Michel-Beyerle, N. Rösch, A quantum chemical study of photoinduced DNA repair: on the splitting of pyrimidine model dimers initiated by electron transfer, J. Am. Chem. Soc. 118 (1996) 9750–9758.
[165] A.A. Voityuk, N. Rösch, Ab initio study on the structure and splitting of the uracil dimer anion radical, J. Phys. Chem., A 101 (1997) 8335–8338.
[166] B. Durbeej, L.A. Eriksson, Thermodynamics of the photoenzymic repair mechanism studied by density functional theory, J. Am. Chem. Soc. 122 (2000) 10126–10132.
[167] N.J. Saettel, O. Wiest, DFT study of the [2+2] cycloreversion of uracil dimer anion radical: waters matter, J. Am. Chem. Soc. 123 (2001) 2693–2694.
[168] M. Schmitz, P. Tavan, M. Nonella, Vibrational analysis of carbonyl modes in different stages of light-induced cyclopyrimidine dimer repair reactions, Chem. Phys. Lett. 349 (2001) 342–348.
[169] A.J. Ramsey, J.L. Alderfer, M.S. Jorns, Energy transduction during catalysis by *Escherichia coli* DNA photolyase, Biochemistry 31 (1992) 7134–7142.
[170] S.-T. Kim, S.D. Rose, Pyrimidine dimer splitting in covalently linked dimer-arylamine systems, J. Photochem. Photobiol., B Biol. 12 (1992) 179–191.
[171] S.-T. Kim, R.F. Hartman, S.D. Rose, Solvent dependence of pyrimidine dimer splitting in a covalently linked dimer-indole system, Photochem. Photobiol. 52 (1990) 789–794.
[172] V. Massey, G. Palmer, On the existence of spectrally distinct classes of flavoprotein semiquinones. A new method for the quantitative production of flavoprotein semiquinones, Biochemistry 5 (1966) 3181–3189.
[173] C.W.M. Kay, E. Schleicher, A. Kuppig, H. Hofner, W. Rüdiger, M. Schleicher, M. Fischer, A. Bacher, S. Weber, G. Richter, Blue light perception in plants. Detection and characterization of a light-induced neutral flavin radical in a C450A mutant of phototropin, J. Biol. Chem. 278 (2003) 10973–10982.
[174] J. Stubbe, D.G. Nocera, C.S. Yee, M.C.Y. Chang, Radical initiation in the class I ribonucleotide reductase: long-range proton-coupled electron transfer? Chem. Rev. 103 (2003) 2167–2201.
[175] P.F. Heelis, T. Okamura, A. Sancar, Excited-state properties of *Escherichia coli* DNA photolyase in the picosecond to millisecond time scale, Biochemistry 29 (1990) 5694–5698.
[176] Y.F. Li, P.F. Heelis, A. Sancar, Active site of DNA photolyase: tryptophan-306 is the intrinsic hydrogen atom donor essential for flavin radical photoreduction and DNA repair in vitro, Biochemistry 30 (1991) 6322–6329.
[177] S.-T. Kim, P.F. Heelis, A. Sancar, Role of tryptophans in substrate binding and catalysis by DNA photolyase, Methods Enzymol. 258 (1995) 319–343.
[178] C.C. Page, C.C. Moser, X. Chen, L. Dutton, Natural engineering principles of electron tunnelling in biological oxidation-reduction, Nature (Lond.) 402 (1999) 47–52.
[179] R. Brudler, K. Hitomi, H. Daiyasu, H. Toh, K.-i. Kucho, M. Ishiura, M. Kanehisa, V.A. Roberts, T. Todo, J.A. Tainer, E.D. Getzoff, Identification of a new cryptochrome class: structure, function, and evolution, Mol. Cell 11 (2003) 59–67.
[180] A.R. Cashmore, J.A. Jarillo, Y.-J. Wu, D. Liu, Cryptochromes: blue light receptors for plants and animals, Science 284 (1999) 760–765.
[181] O. Froy, D.C. Chang, S.M. Reppert, Redox potential: differential roles in dCRY and mCRY1 functions, Curr. Biol. 12 (2002) 147–152.
[182] M. Byrdin, A.P.M. Eker, M.H. Vos, K. Brettel, Dissection of the triple tryptophan electron transfer chain in *Escherichia coli* DNA photolyase: Trp382 is the primary donor in photoactivation, Proc. Natl. Acad. Sci. U. S. A. 100 (2003) 8676–8681.
[183] T. Okamura, A. Sancar, P.F. Heelis, Y. Hirata, N. Mataga, Doublet-quartet intersystem crossing of flavin radical in DNA photolyase, J. Am. Chem. Soc. 111 (1989) 5967–5969.
[184] C. Aubert, M.H. Vos, P. Mathis, A.P.M. Eker, K. Brettel, Intraprotein radical transfer during photoactivation of DNA photolyase, Nature (Lond.) 405 (2000) 586–590.
[185] P.F. Heelis, A. Sancar, T. Okamura, Excited quartet states in DNA photolyase, J. Photochem. Photobiol., B Biol. 16 (1992) 387–390.
[186] D.M. Popovic, A. Zmiric, S.D. Zaric, E.-W. Knapp, Energetics of radical transfer in DNA photolyase, J. Am. Chem. Soc. 124 (2002) 3775–3782.
[187] M.S. Cheung, I. Daizadeh, A.A. Stuchebrukhov, P.F. Heelis, Pathways of electron transfer in *Escherichia coli* DNA photolyase: Trp306 to FADH, Biophys. J. 76 (1999) 1241–1249.
[188] C. Aubert, P. Mathis, A.P.M. Eker, K. Brettel, Intraprotein electron transfer between tyrosine and tryptophan in DNA photolyase from *Anacystis nidulans*, Proc. Natl. Acad. Sci. U. S. A. 96 (1999) 5423–5427.

[189] C. Aubert, K. Brettel, P. Mathis, A.P.M. Eker, A. Boussac, EPR detection of the transient tyrosyl radical in DNA photolyase from *Anacystis nidulans*, J. Am. Chem. Soc. 121 (1999) 8659–8660.
[190] C. Essenmacher, S.-T. Kim, M. Atamian, G.T. Babcock, A. Sancar, Tryptophan radical formation in DNA photolyase: electron-spin polarization arising from photoexcitation of a doublet ground state, J. Am. Chem. Soc. 115 (1993) 1602–1603.
[191] S.-T. Kim, A. Sancar, C. Essenmacher, G.T. Babcock, Time-resolved EPR studies with DNA photolyase: excited-state $FADH^0$ abstracts an electron from Trp-306 to generate $FADH^-$, the catalytically active form of the cofactor, Proc. Natl. Acad. Sci. U. S. A. 90 (1993) 8023–8027.
[192] T. Mizukoshi, K. Hitomi, T. Todo, S. Iwai, Studies on the chemical synthesis of oligonucleotides containing the (6–4) photoproduct of thymine-cytosine and its repair by (6–4) photolyase, J. Am. Chem. Soc. 120 (1998) 10634–10642.
[193] A. Joseph, G. Prakash, D.E. Falvey, Model studies of the (6–4) photoproduct photolyase enzyme: laser flash photolysis experiments confirm radical ion intermediates in the sensitized repair of thymine oxetane adducts, J. Am. Chem. Soc. 122 (2000) 11219–11225.
[194] A. Joseph, D.E. Falvey, Photoinduced electron transfer cleavage of oxetane adducts of uracil and cytosine, Photochem. Photobiol. Sci. 1 (2002) 632–635.
[195] P.F. Heelis, S. Liu, Photoenzymic repair of the DNA 6–4 photoproduct—a density functional theory and semiempirical study, J. Am. Chem. Soc. 119 (1997) 2936–2937.
[196] K. Hitomi, H. Nakamura, S.-T. Kim, T. Mizukoshi, T. Ishikawa, S. Iwai, T. Todo, Role of two histidines in the (6–4) photolyase reaction, J. Biol. Chem. 276 (2001) 10103–10109.
[197] S. Weber, C.W.M. Kay, H. Mögling, K. Möbius, K. Hitomi, T. Todo, Photoactivation of the flavin cofactor in *Xenopus laevis* (6–4) photolyase: observation of a transient tyrosyl radical by time-resolved electron paramagnetic resonance, Proc. Natl. Acad. Sci. U. S. A. 99 (2002) 1319–1322.
[198] M. Fuchs, E. Schleicher, A. Schnegg, C.W.M. Kay, J.T. Törring, R. Bittl, A. Bacher, G. Richter, K. Möbius, S. Weber, The g-tensor of the neutral flavin radical cofactor of DNA photolyase revealed by 360-GHz electron paramagnetic resonance spectroscopy, J. Phys. Chem., B 106 (2002) 8885–8890.
[199] S. Un, X.S. Tang, B.A. Diner, 245 GHz high-field EPR study of tyrosine-D^0 and tyrosine-Z^0 in mutants of photosystem II, Biochemistry 35 (1996) 679–684.
[200] G. Bleifuss, M. Kolberg, S. Pötsch, W. Hofbauer, R. Bittl, W. Lubitz, A. Gräslund, G. Lassmann, F. Lendzian, Tryptophan and tyrosine radicals in ribonucleotide reductase: a comparative high-field EPR study at 94 GHz, Biochemistry 40 (2001) 15362–15368.
[201] H. Stege, L. Roza, A.A. Vink, M. Grewe, T. Ruzicka, S. Grether-Beck, J. Krutmann, Enzyme plus light therapy to repair DNA damage in ultraviolet-B-irradiated human skin, Proc. Natl. Acad. Sci. U. S. A. 97 (2000) 1790–1795.